Diffusion and Diffusion creep...

1. Introduction: Observations of textures associated with pressure solution and diffusion creep

2. Theoretical description of Diffusion:
a. Random walk
b. continuum theory.
  -driven by concentration gradients
  -driven by stress gradients

3. Diffusion Pathways: Diffusivity and Diffusion paths and a word on Grain boundaries.

4. Models for diffusion creep in rocks at high temperature:
Lattice and grain boundary diffusion creep...

5. Experimental data: Rheological data for olivine

6. Effects of Water

7. Effects of Melt
-Coble Creep, Cooper-Kohlstedt model, Contiguity model

1. Intro: Observations

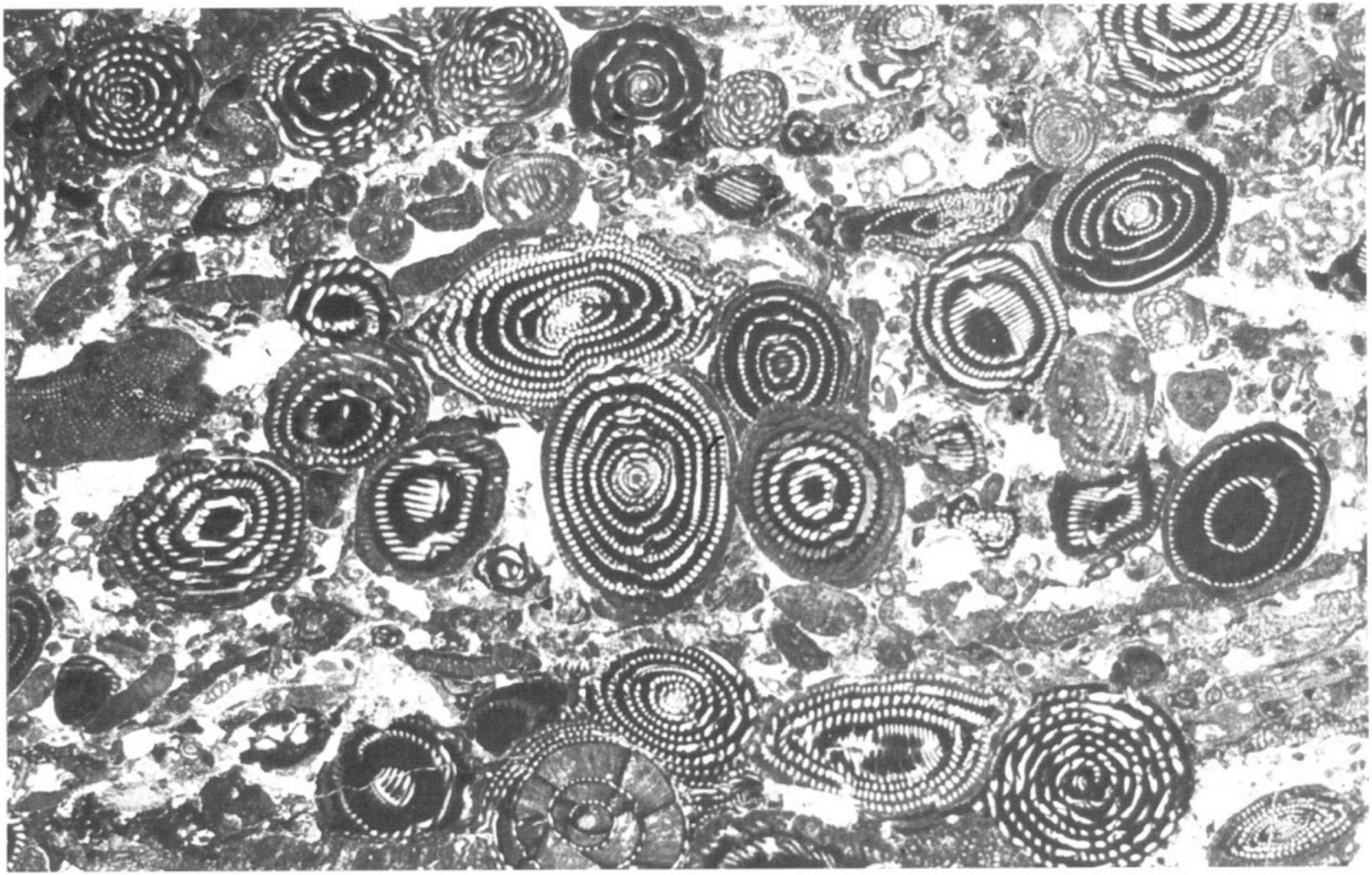

Fig. 3.4. Numulitic limestone showing evidence for stress-induced solution transfer during diagenetic compaction. The four fossils in the *centre* show indentation by dissolution and minor ductile deformation as a result of vertical shortening. Eastern Pyrenees, Spain. Width of view 21 mm. PPL

from: “Microtectonics”

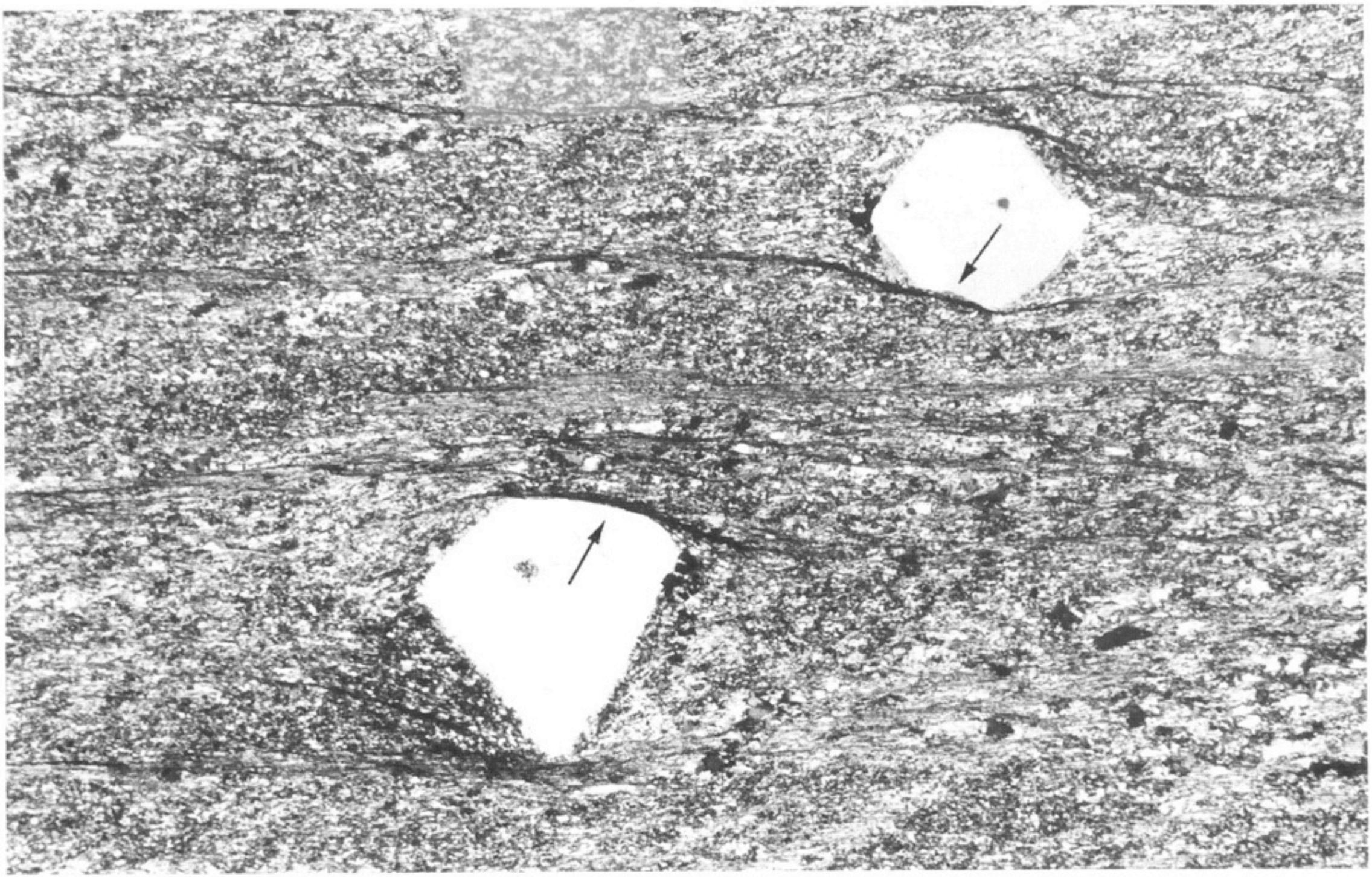

Fig. 3.3. Dissolution of single idiomorphic quartz crystals *(arrows)* in an ignimbrite. ***Dark horizontal seams*** consist of insoluble material that became concentrated during dissolution. Leonora, Yilgarn Craton, Australia. Width of view 4 mm. PPL

from: “Microtectonics”

Calcite mylonite

straight boundaries,
triple and 4 grain jcns
weakly elongated grains
uniform grain size

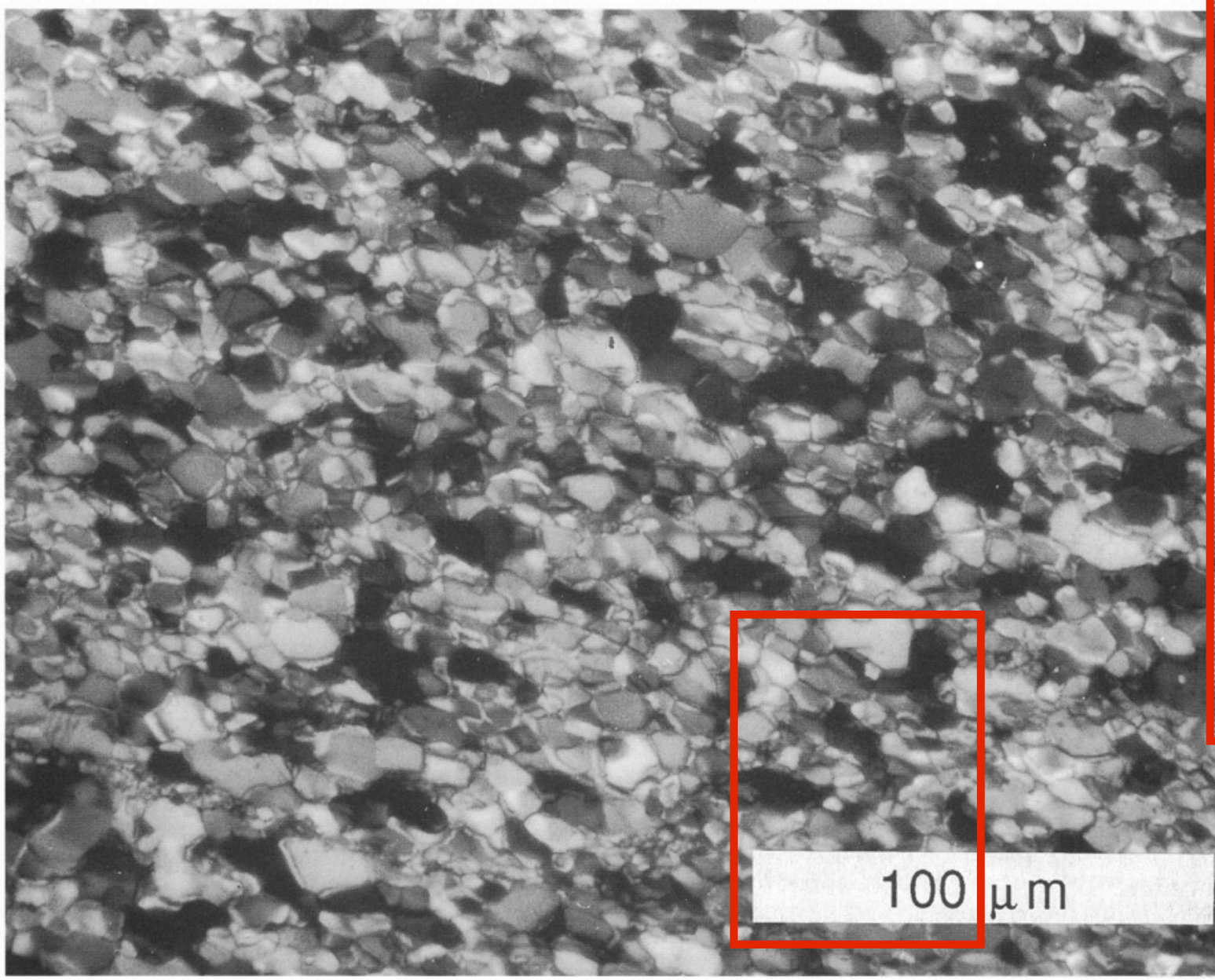

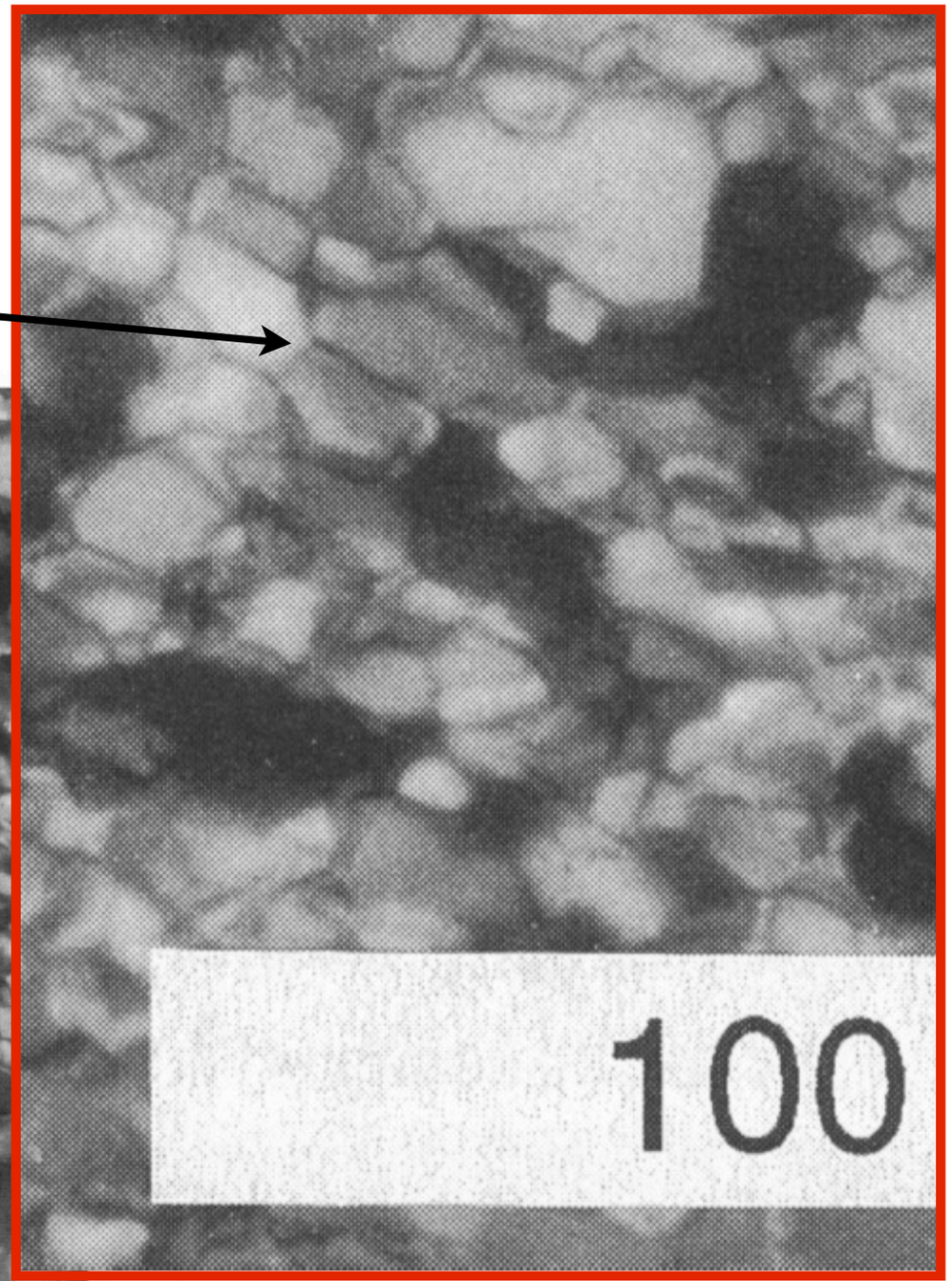

from:
"Fault-related Rocks:
A Photographic Atlas"

Mylonite with Ultramylonite (um) derived from granite (S. California):

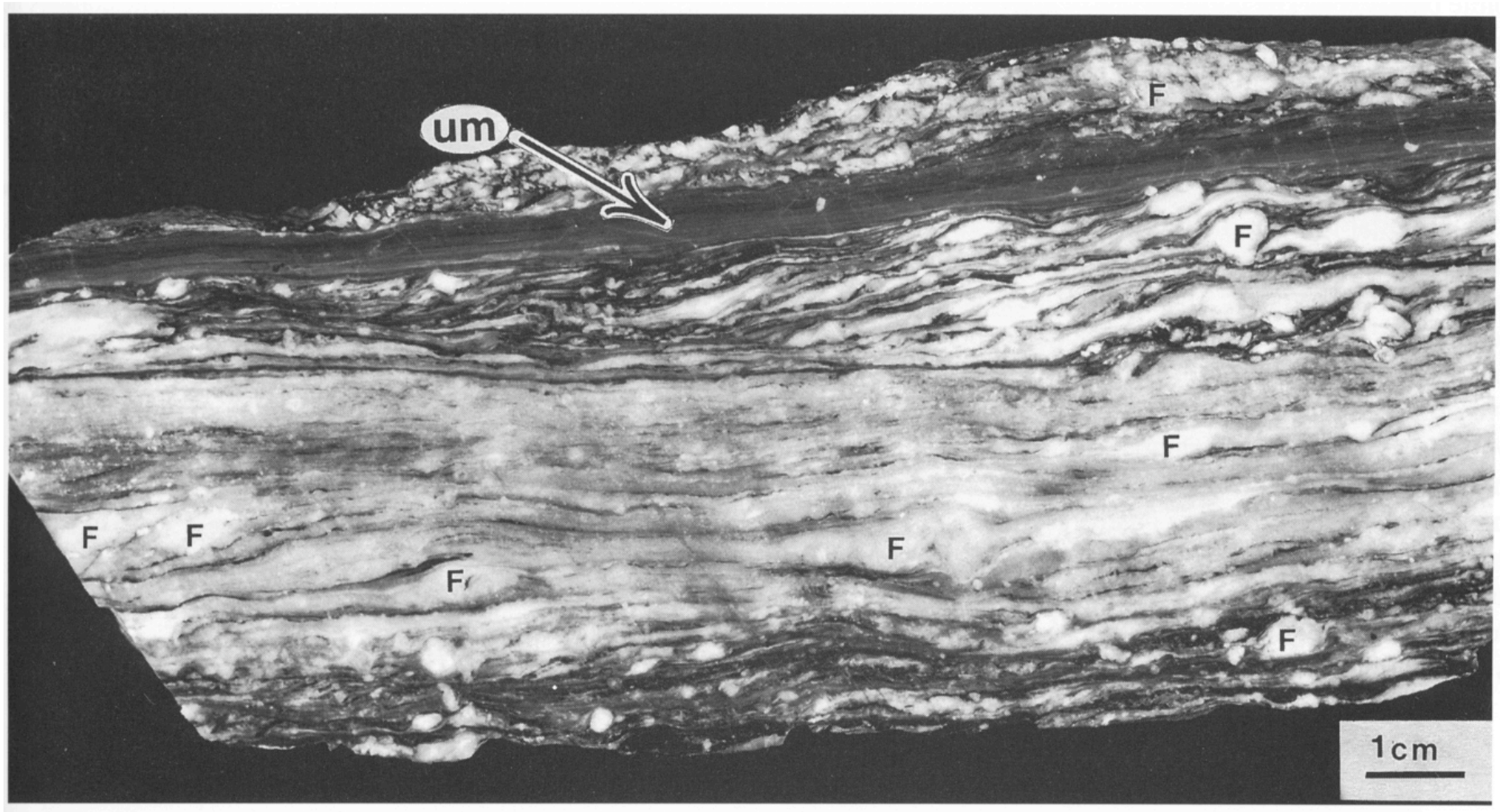

64

from:
"Fault-related Rocks:
A Photographic Atlas"

2. Theoretical descriptions of diffusion

1. Random walk: diffusion is a random walk process (when, in the presence of a gradient, gives a flux down that gradient)

2. Can be described by a continuum behavior: Fick's first law (the delta spike decay).

3. Fick's second law (1st Law + continuity eqn)

4. Generalized to any gradient ? Stress gradient (or electromagnetic, eg)? How does stress drive diffusion ?

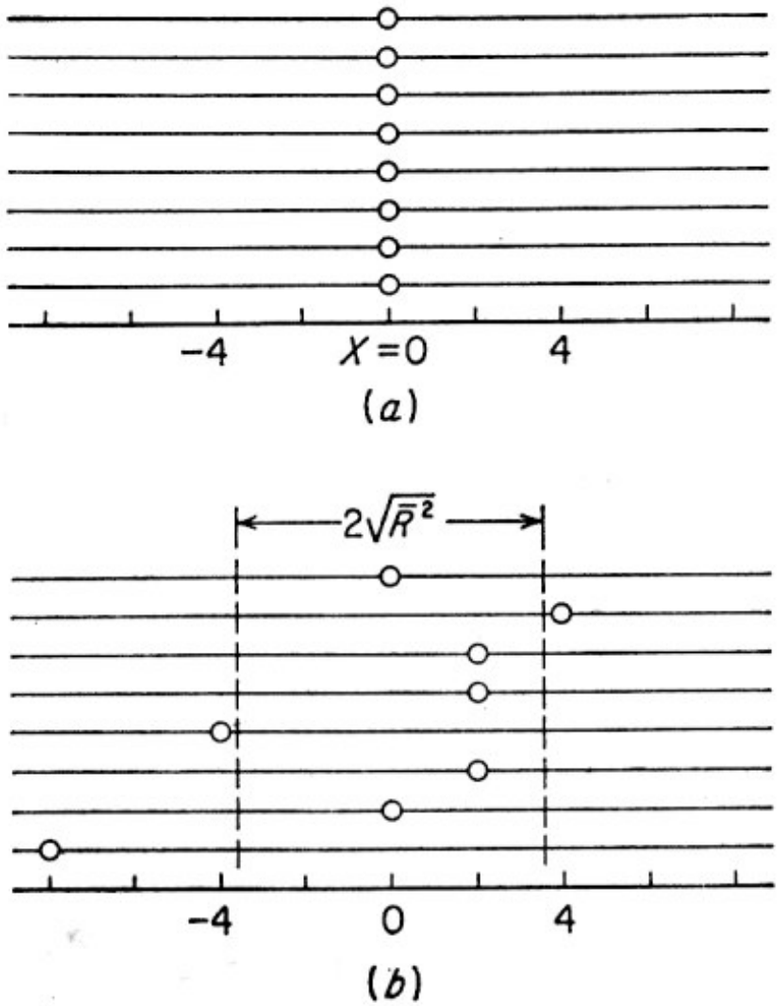

FIG. 2-9. (*a*) Initial distribution of atoms, one to a line. (*b*) Final distribution after each atom took 16 random jumps. $\sqrt{\overline{R^2}}$ is the calculated root mean square for the points shown.

from:Shewmon

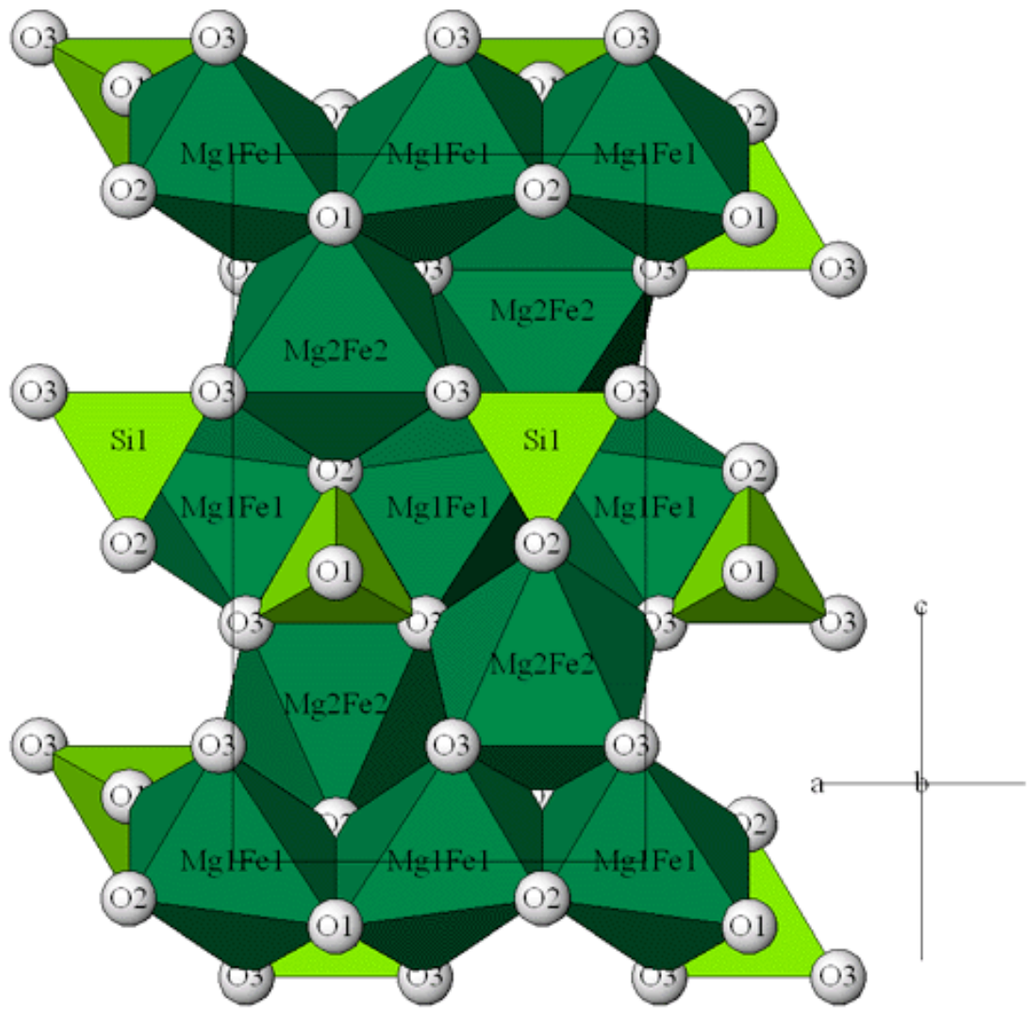

on a lattice, these jumps are limited to “sublattices”

http://en.wikipedia.org/wiki/Atomic_diffusion

http://www.youtube.com/watch?v=QfQolcXrV1M&NR=1

http://www.youtube.com/watch?v=xDIyAOBa_yU

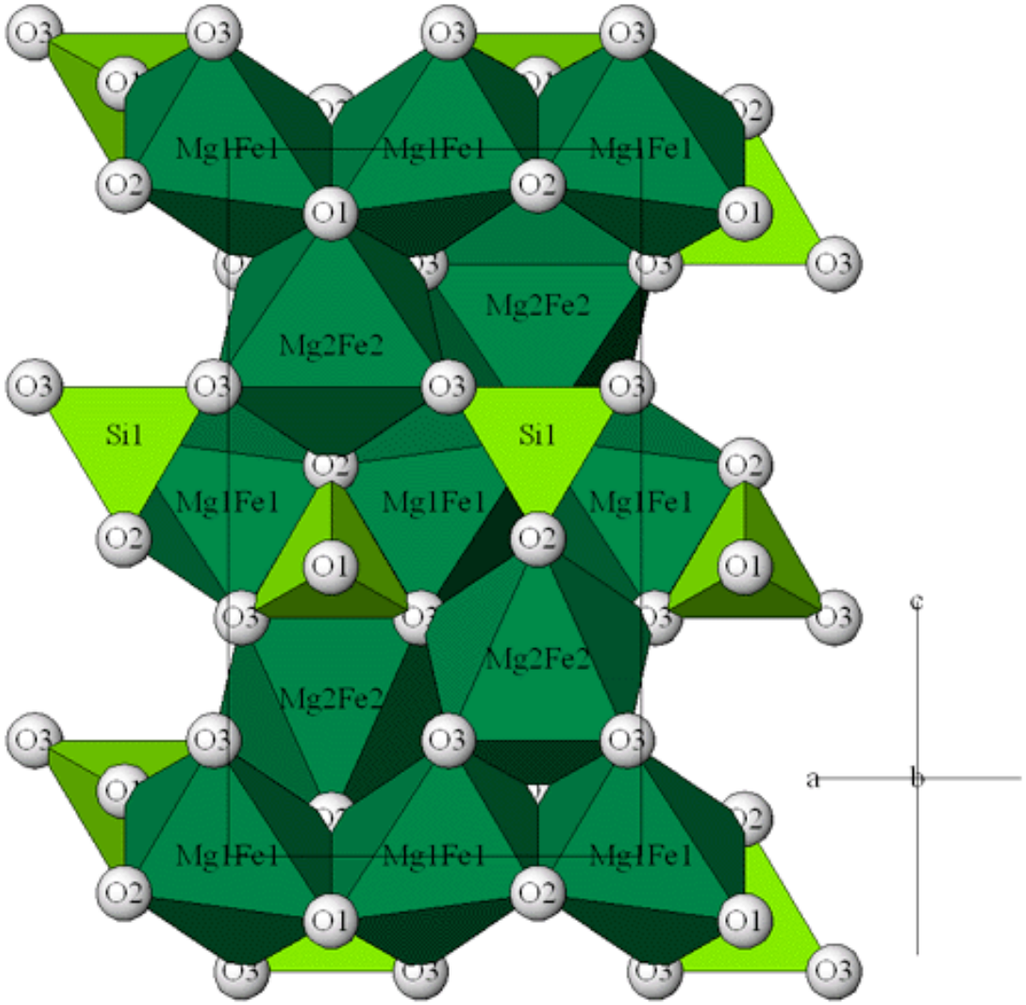

http://staff.aist.go.jp/nomura-k/english/itscgallary-e.htm

random walk (Karato, Ch. 8):

$$D = \frac{1}{c.n.} a^2 \Gamma$$

$$\Gamma = X_d \Gamma_m$$

$$\Gamma_m = \nu \exp\left(\frac{-G_m}{RT}\right)$$

$$D = \frac{1}{c.n.} a^2 \nu \exp\left(\frac{-G_m}{RT}\right)$$

Γ is a probability of migrating.

ν is the lattice vibration frequency

$$J_i = -J_v$$

$$X_i D_i = X_v D_v$$

$$X_i = 1 - X_v \approx 1$$

$$D_i \approx X_v D_v$$

The equilibrium concentration of vacancies

$$S_{conf} = -k_B \ln W$$

Maxwell-Boltzmann Statistical Thermodynamics:

$$W = \left[\frac{(N+n_v)!}{N!n_v!}\right]$$

$$G(T,P,N,n_v) = G_0(T,P) + n_v g_v^f - k_B T \ln W$$

$$G(T,P,N,n_v) = G_0(T,P) + n_v g_v^f - k_B T \ln \left[\frac{(N+n_v)!}{N!n_v!}\right]$$

$$\left(\frac{\partial G}{\partial n_v}\right)_{(T,P)} = g_v^f - k_B T \frac{\partial}{\partial n_v} \ln W$$

$$\left(\frac{\partial G}{\partial n_v}\right)_{(T,P)} = g_v^f - k_B T \frac{\partial}{\partial n_v} \ln \left[\frac{(N+n_v)!}{N!n_v!}\right]$$

$$\left(\frac{\partial G}{\partial n_v}\right)_{(T,P)} = g_v^f - k_B T \ln \left(\frac{n_v}{N+n_v}\right)$$

$$\left(\frac{\partial G}{\partial n_v}\right)_{(T,P)} = g_v^f - k_B T \ln (X_v)$$

$$\left(\frac{\partial G}{\partial n_v}\right) = 0$$

$$X_v^{eq} = \exp\left(\frac{g_v^f}{k_B T}\right)$$

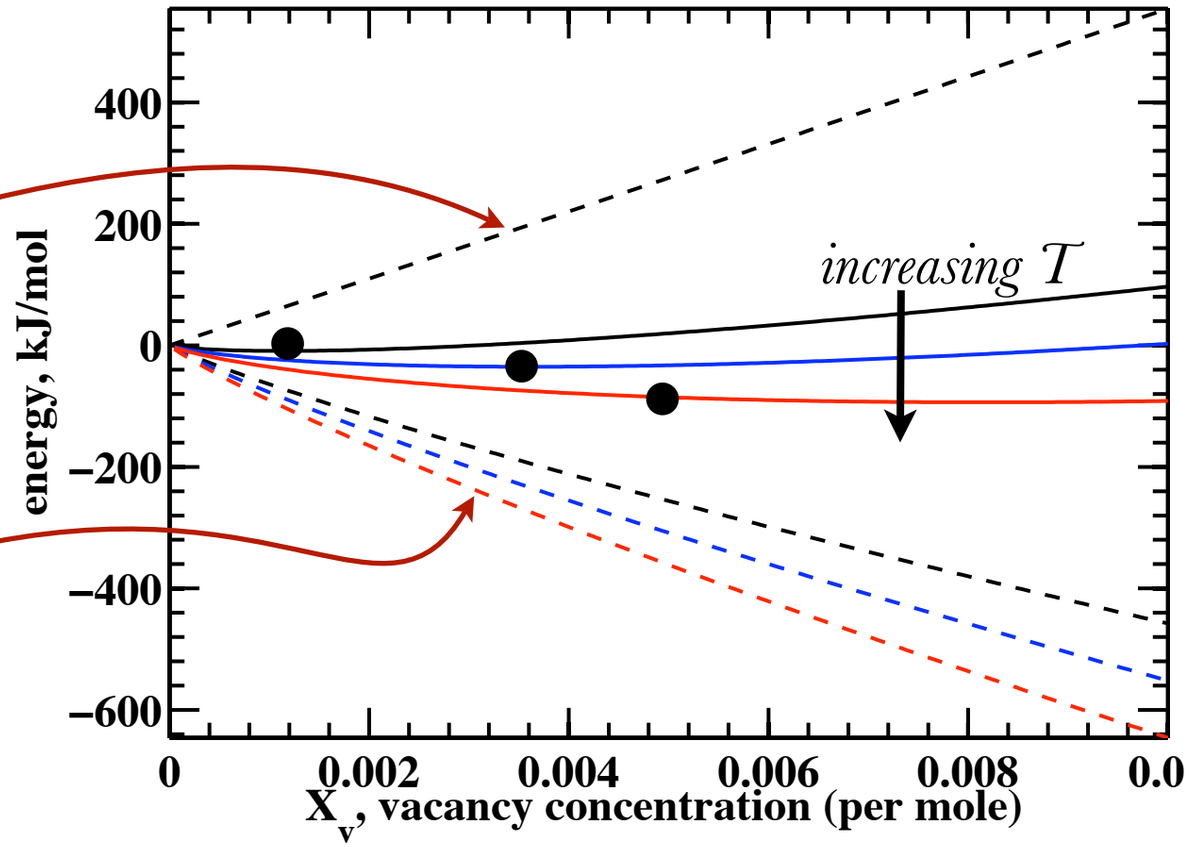

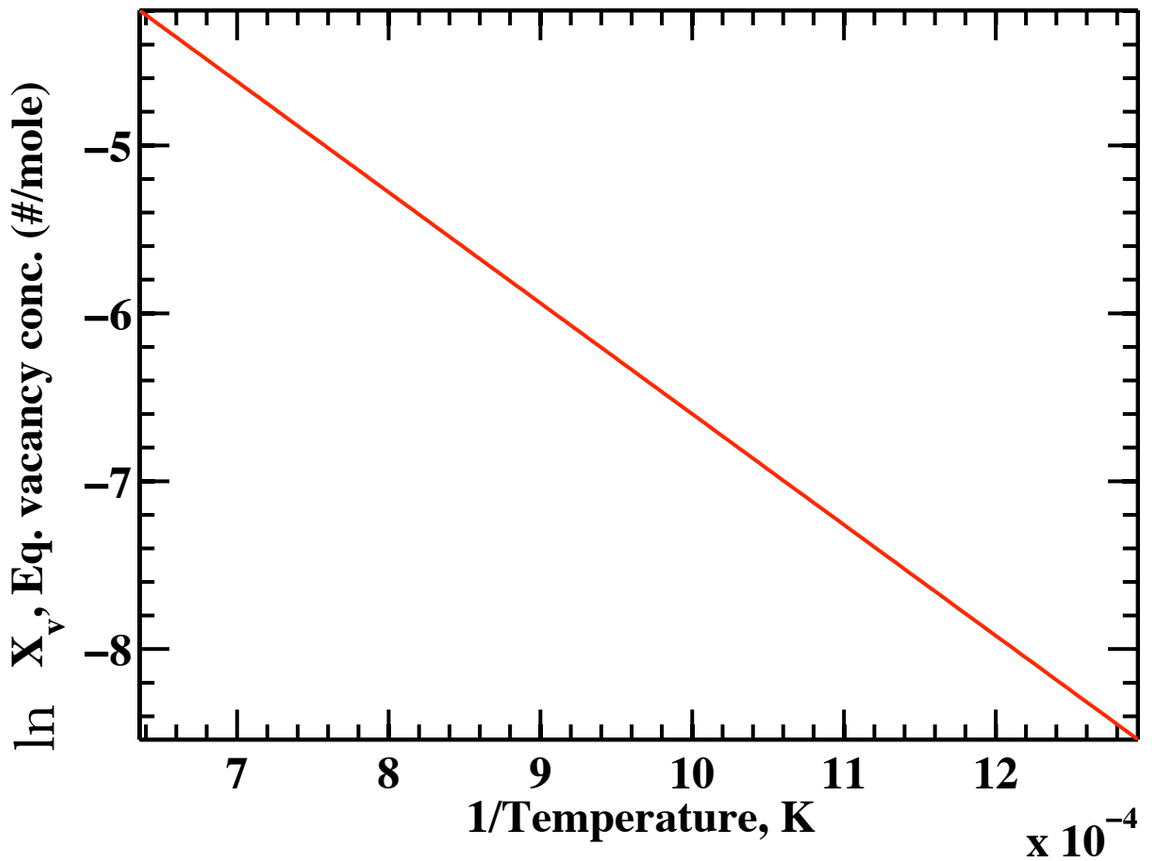

CONTINUUM VIEW: a tracer between two rods:

Fick's 1st Law: $J = -D\nabla c$

"continuity" eqn:

$$\frac{\partial c}{\partial t} = -\nabla J$$

$$(J = -D\nabla c)$$

$$\frac{\partial c}{\partial t} = -\nabla\left(-D\nabla c\right)$$

$$\frac{\partial c}{\partial t} = D\nabla^2 c$$

Fick's 2nd Law

$$J = -D_i\left(\frac{\partial c_i}{\partial x}\right)$$

$$\frac{\partial c}{\partial t} = D_i\left(\frac{\partial^2 c_i}{\partial x^2}\right)$$

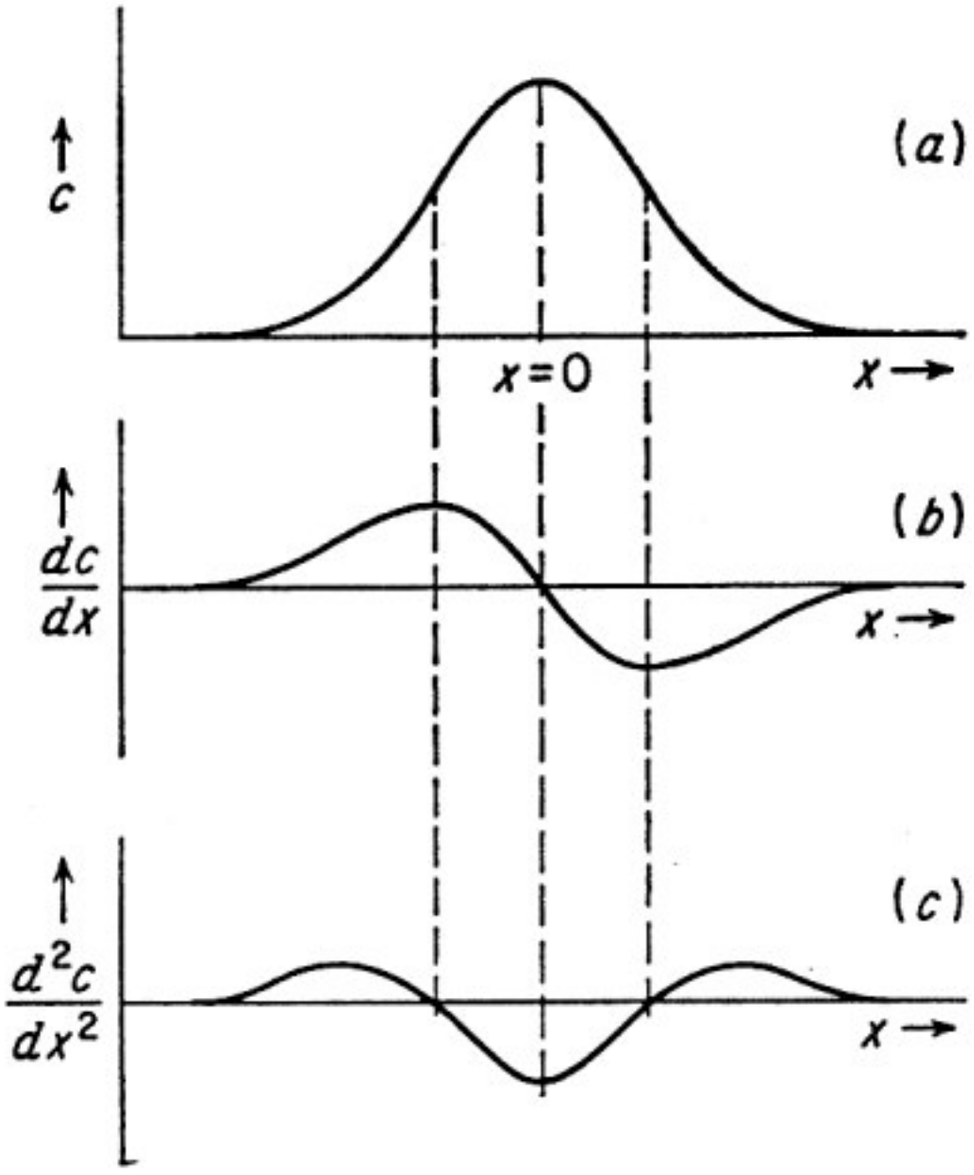

FIG. 1-3. (*a*), (*b*), and (*c*) show $c(x)$, dc/dx versus x, and d^2c/dx^2 versus x, respectively, in arbitrary units for Eq. (1-14).

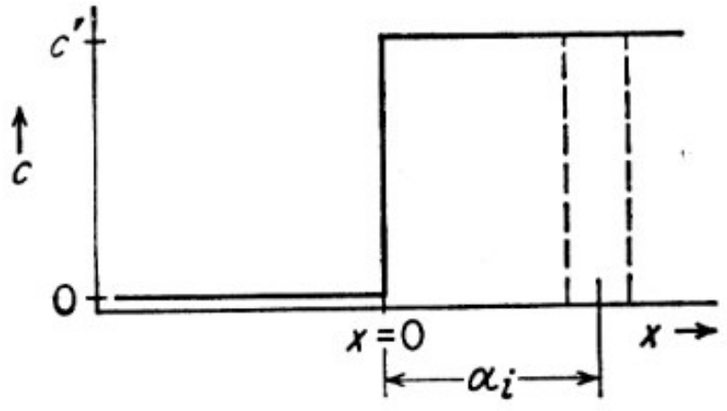

FIG. 1-4

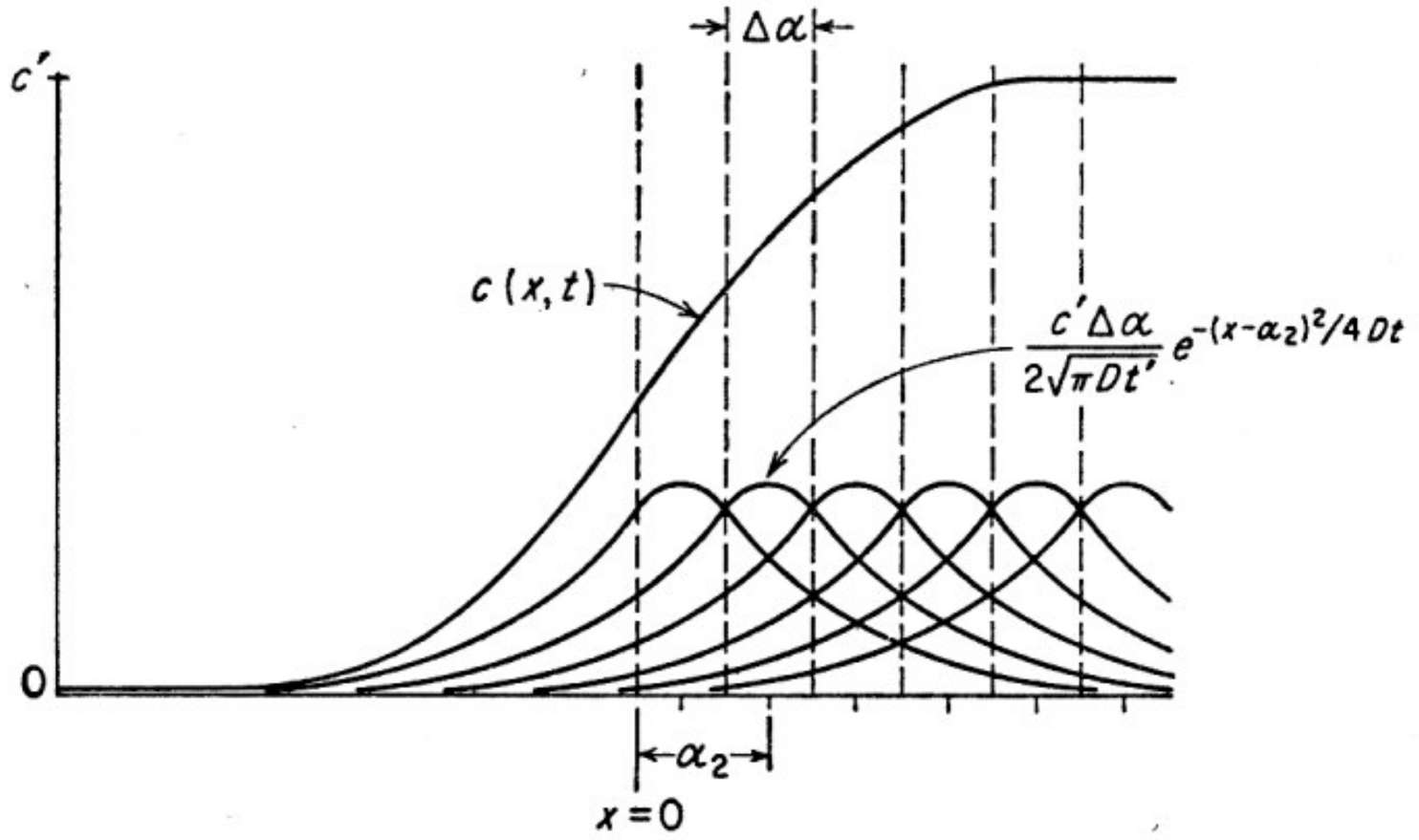

FIG. 1-5. $c(x,t)$ is the sum of the exponential curves which represent the sol diffusing out of each slab $\Delta\alpha$ thick.

$$c(x,t) \simeq \frac{c'}{2\sqrt{\pi Dt}} \sum_{i=1}^{n} \Delta\alpha_i \exp\left[-\frac{(x-\alpha_i)^2}{4Dt}\right]$$

Influence of hydrogen on Fe–Mg interdiffusion in (Mg,Fe)O and implications for Earth's lower mantle

Sylvie Demouchy · Stephen J. Mackwell · David L. Kohlstedt

Contrib Mineral Petrol (2007) 154:279–289
DOI 10.1007/s00410-007-0193-9

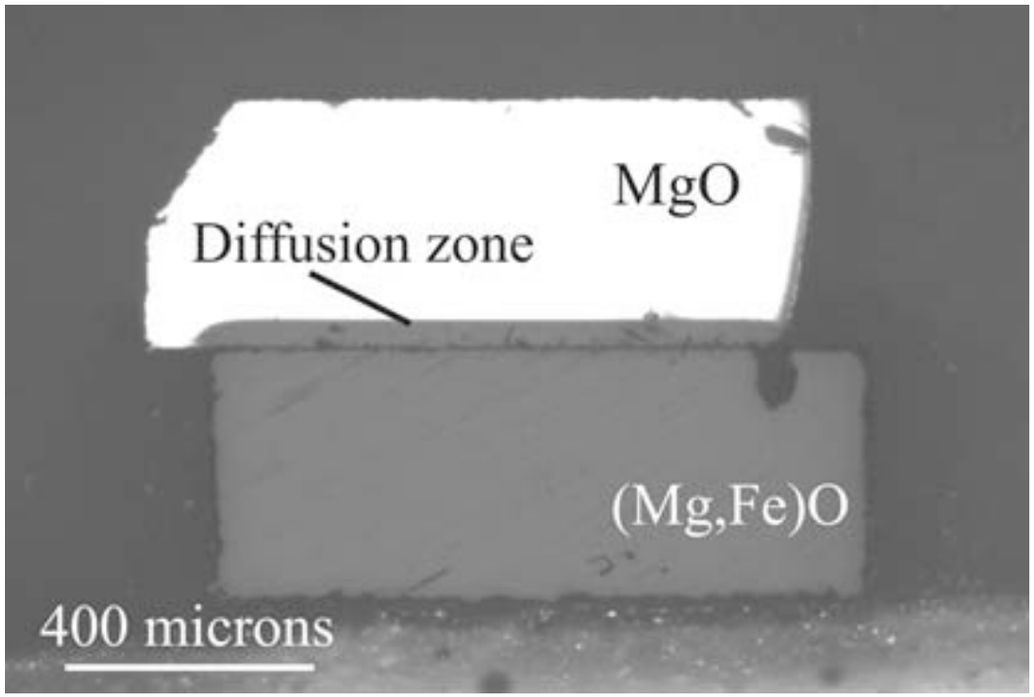

Fig. 1 Photomicrograph of a diffusion couple after a interdiffusion experiment (PI-1238) at 1,200°C

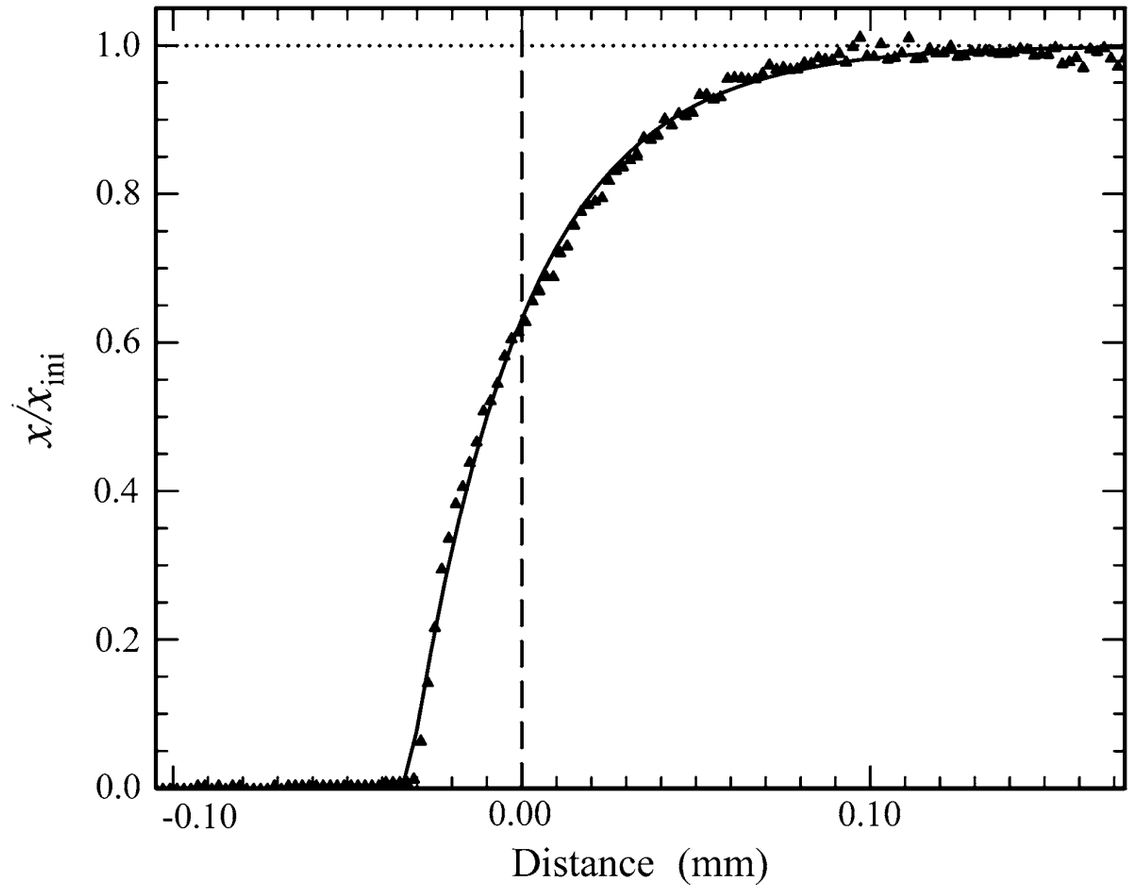

Fig. 2 Concentration profile (x = Fe/(Fe + Mg)) of a sample (PI-1240), annealed at 300 MPa, 1,250°C for 2 h, as a function of the position in the diffusion couple perpendicular to the original interface. Initial interface is set at $z = 0$. The *solid line* shows the non-linear least square fit to the data

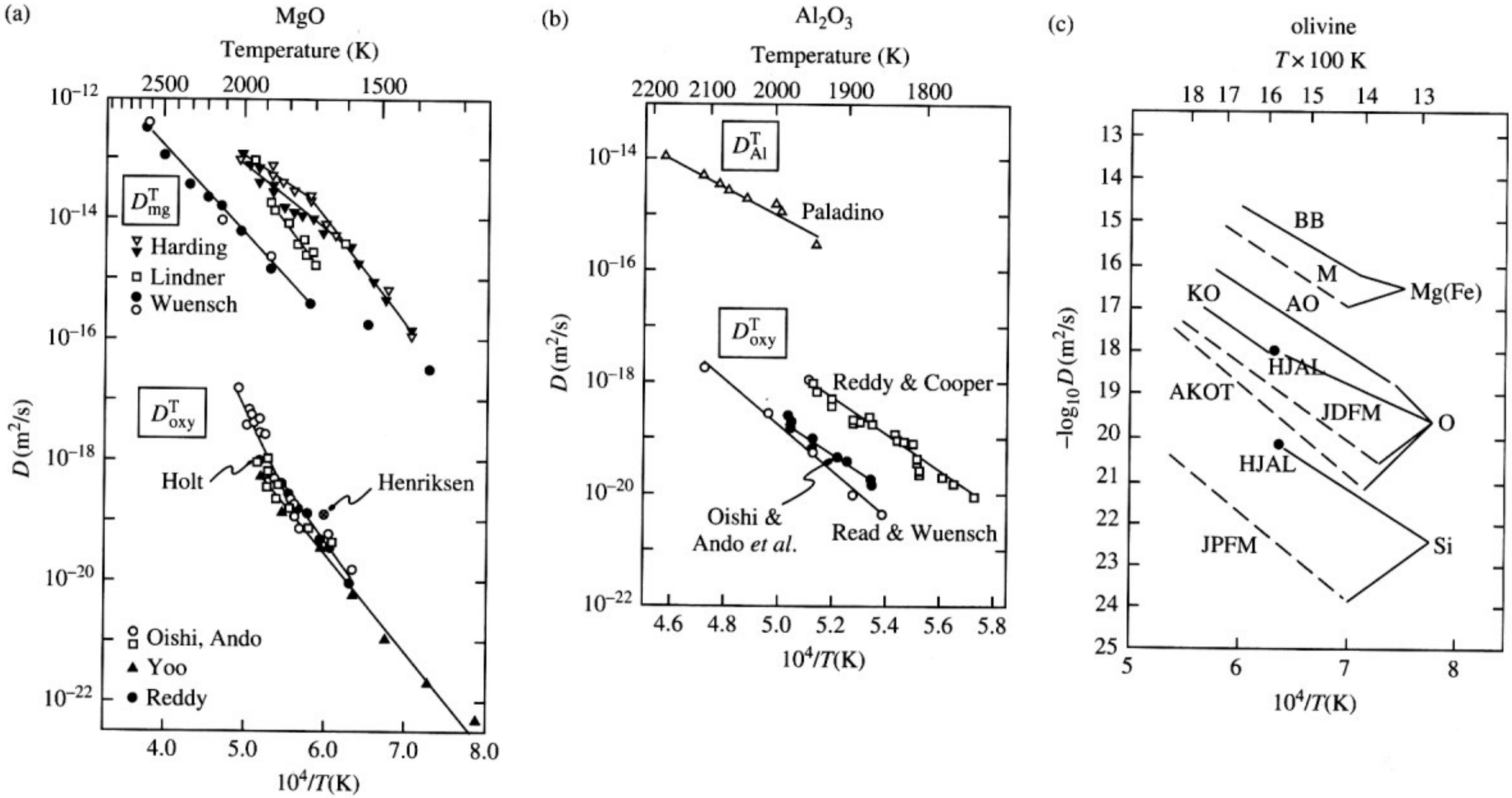

FIGURE 8.2 Self-diffusion coefficients of several ionic species in single crystals of MgO, Al_2O_3 and olivine: (a) MgO (ANDO, 1989), (b) Al_2O_3 (ANDO, 1989), (c) olivine (KARATO, 1989a).

Stress-driven diffusion

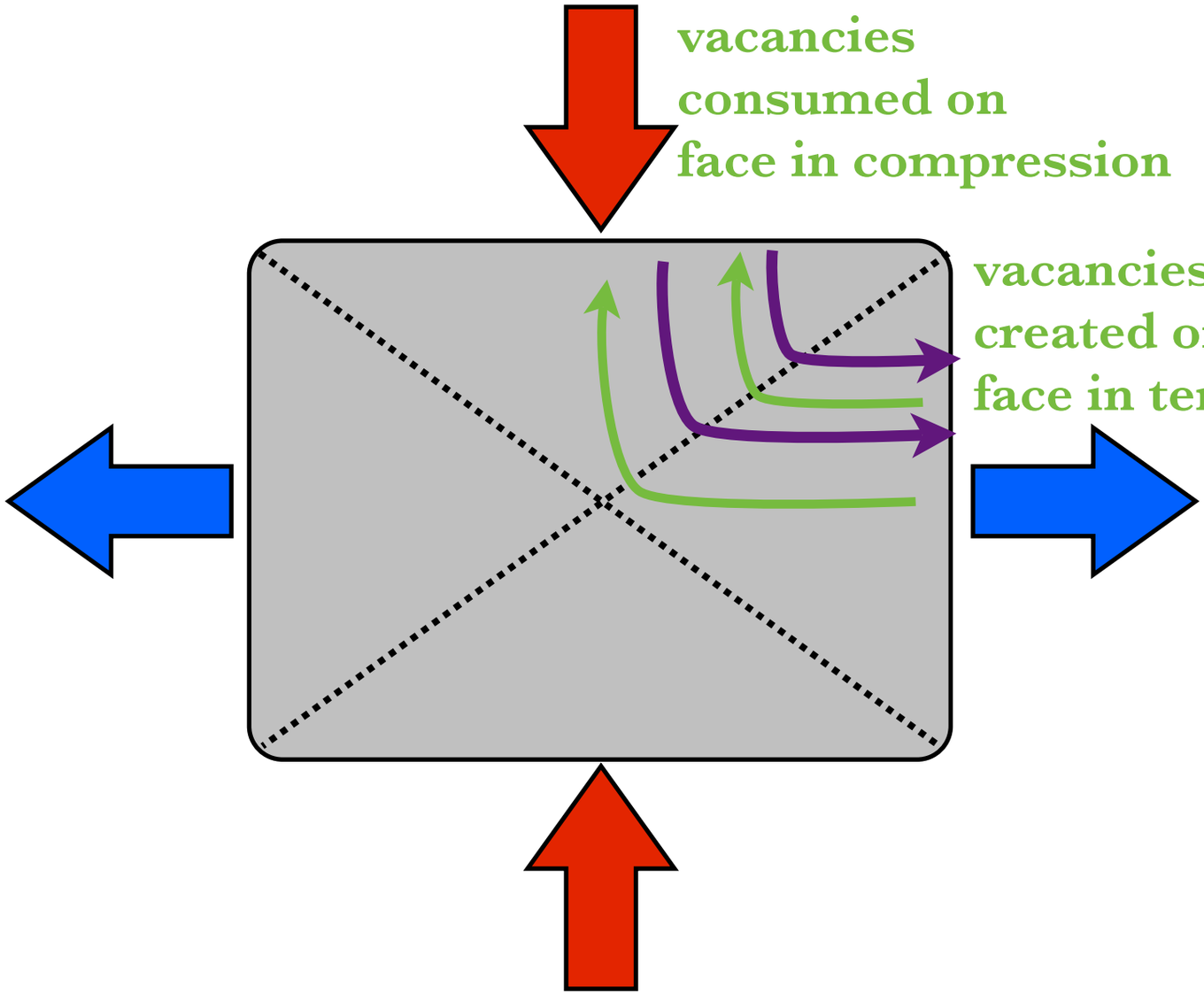

stress effect on chemical potential:

$$\mu_i = \mu_i^0(T) + \Omega_i \sigma_n$$

$$\nabla \mu_i = \Omega_i \nabla \sigma_n$$

$$\nabla \sigma_n \approx (\sigma_{11} - \sigma_{33})/l = \sigma'/l$$

$$J = -D\nabla\mu \approx -D\Omega_i \nabla\sigma$$

atom flux in opposite direction as vacancy flux:

$$J_i = -J_v$$

Stress-induced Al–Cr zoning of spinel in deformed peridotites

Kazuhito Ozawa

Geological Institute, Faculty of Science, University of Tokyo, Tokyo 113, Japan

NATURE · VOL 338 · 9 MARCH 1989

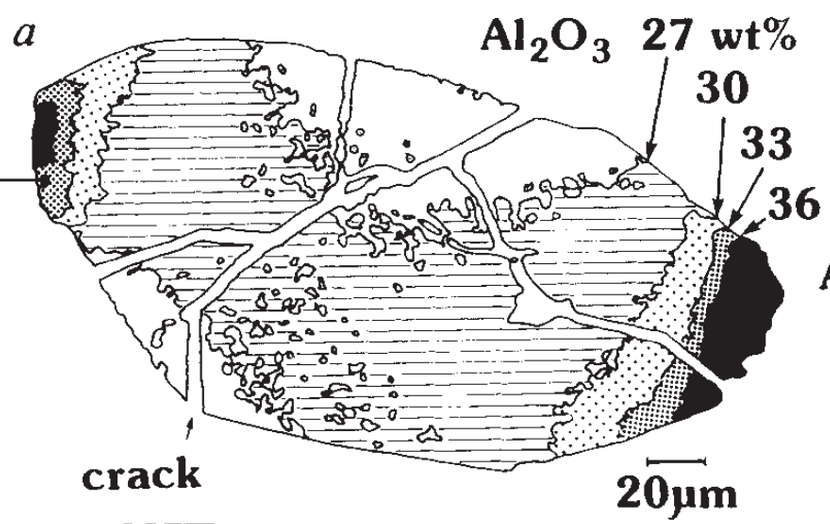

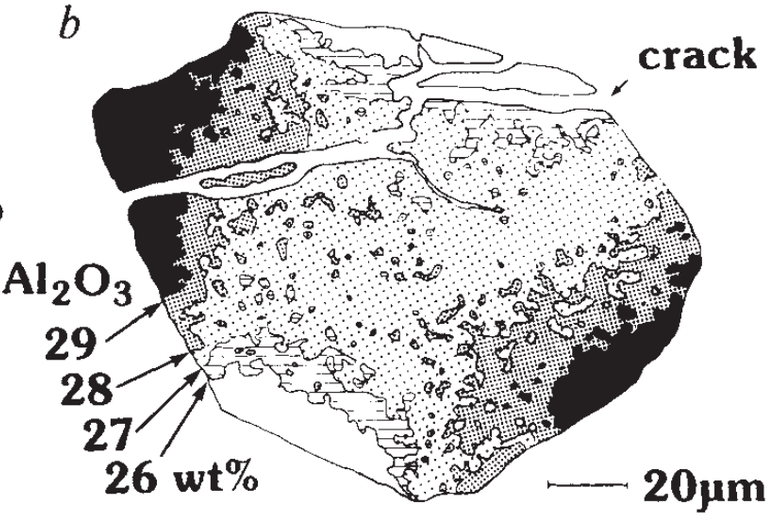

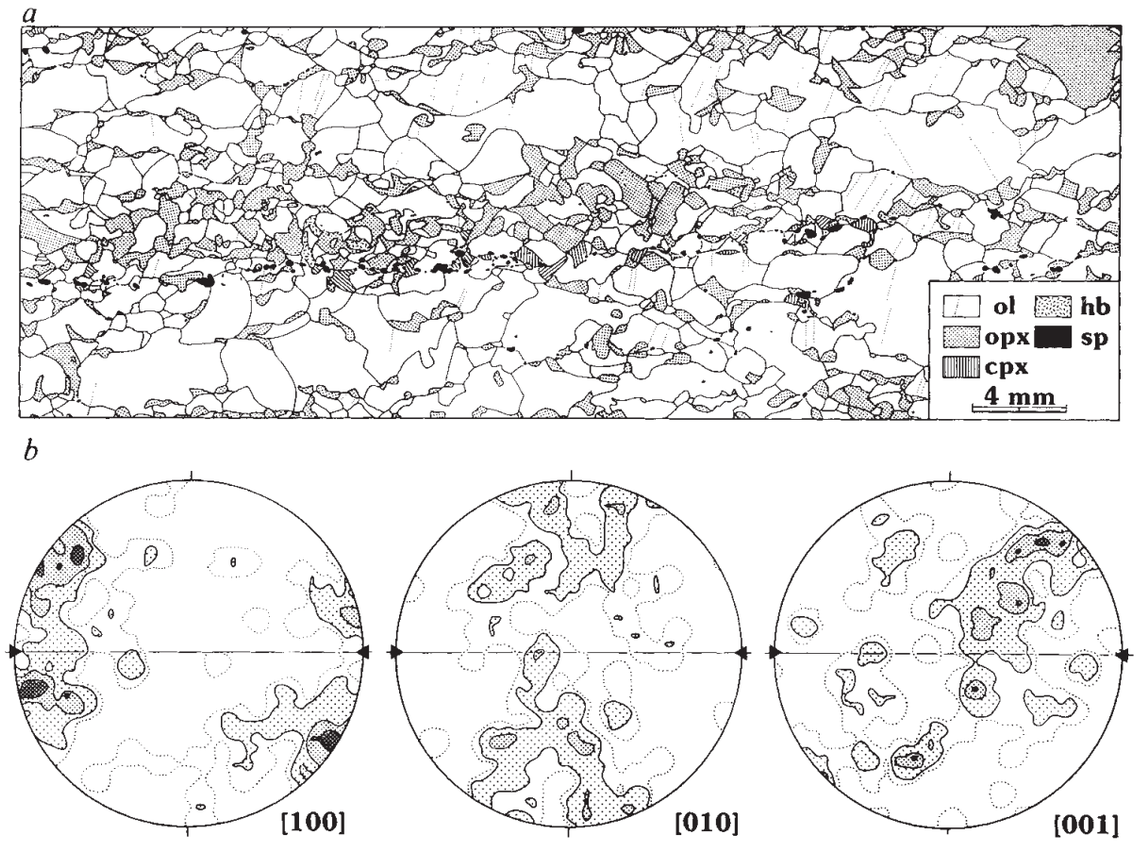

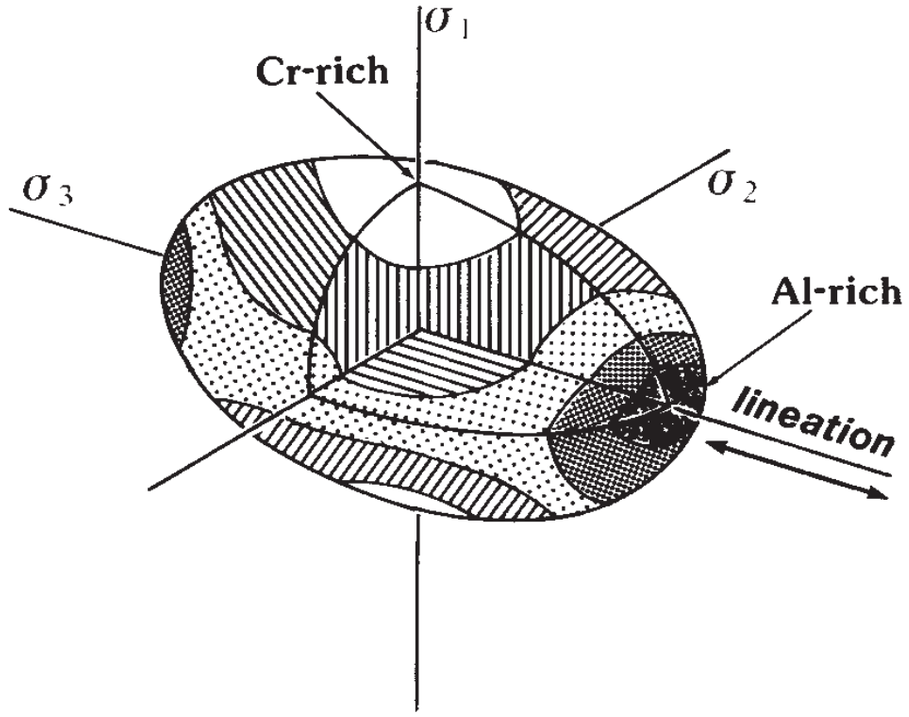

FIG. 4 Schematic picture of three-dimensional multi-polar Al–Cr zoning in spinel. Aluminium concentration decreases through densely stippled, sparsely stippled, and hatched to blank areas. The expected orientation of the three principal stress axes is also shown.

3. Diffusion pathways

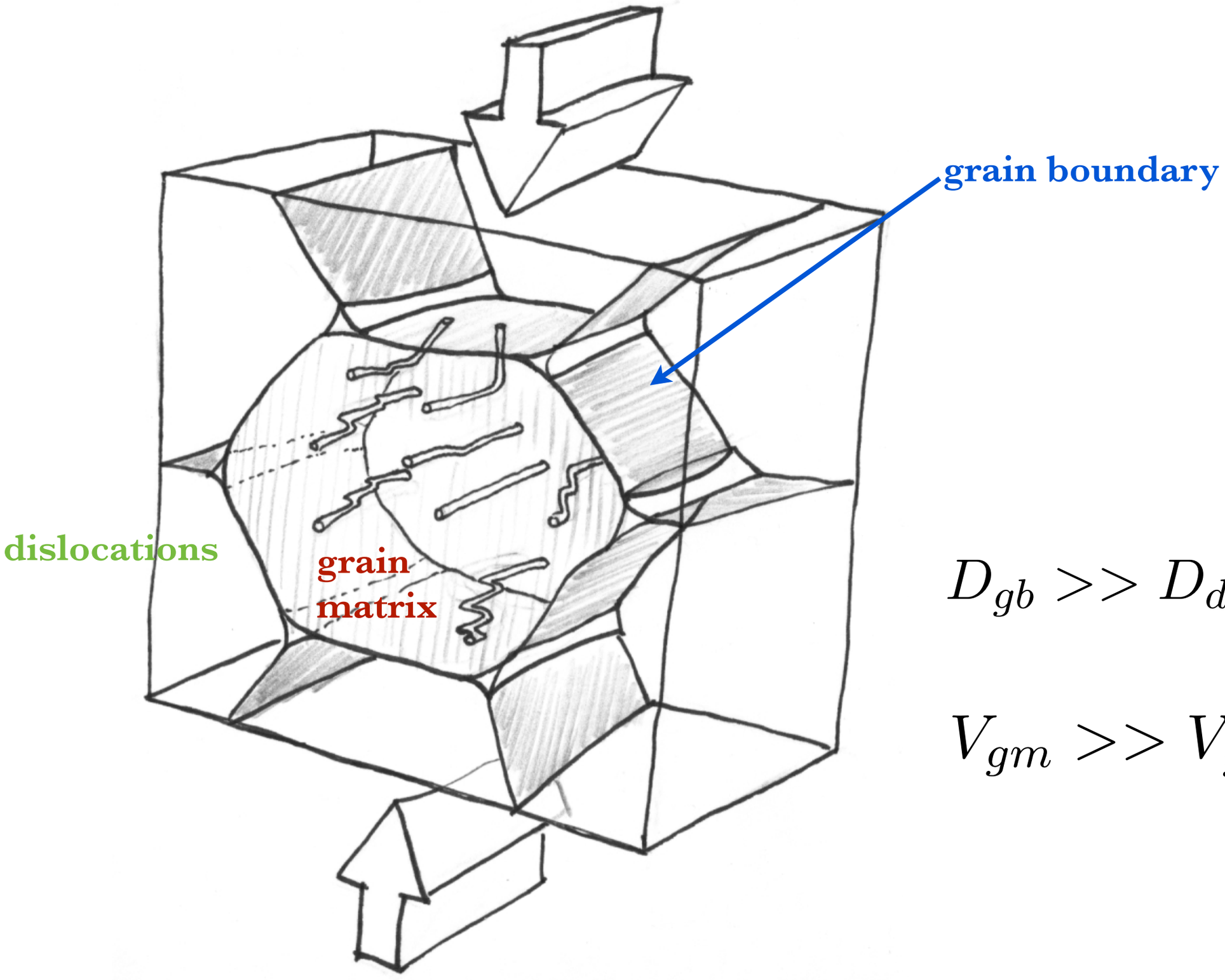

$$D_{gb} >> D_{dis} > D_{gm}$$

$$V_{gm} >> V_{gb} > V_{dis}$$

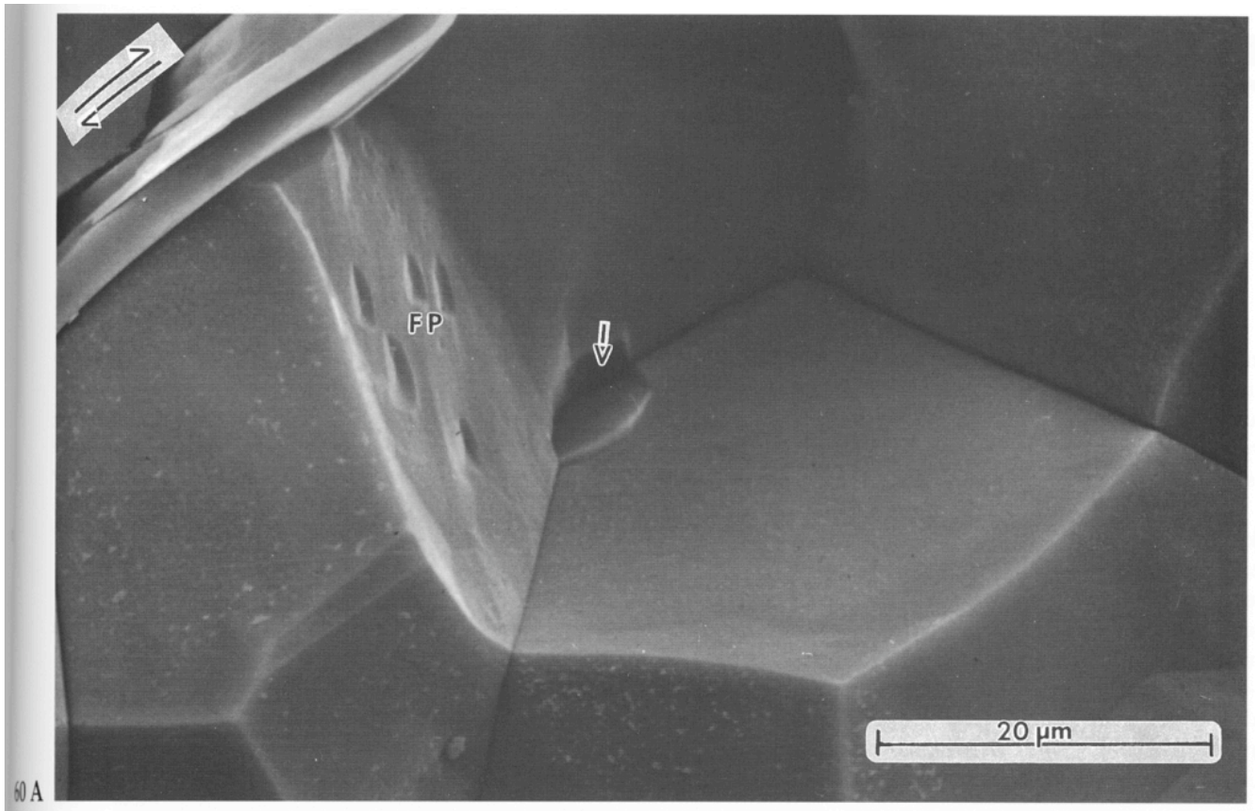

60 A

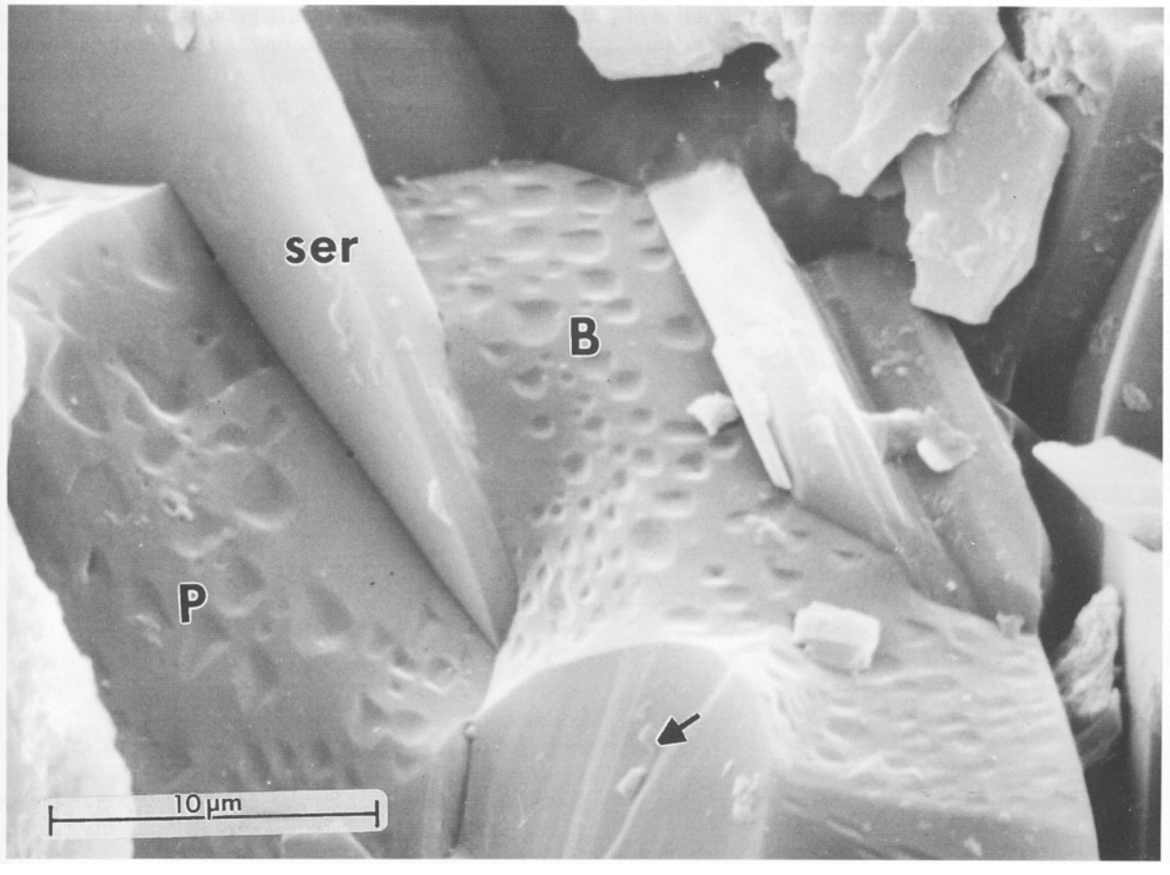

60 B

T. Hiraga · T. Nagase · M. Akizuki

The structure of grain boundaries in granite-origin ultramylonite studied by high-resolution electron microscopy

Phys Chem Minerals (1999) 26: 617–623

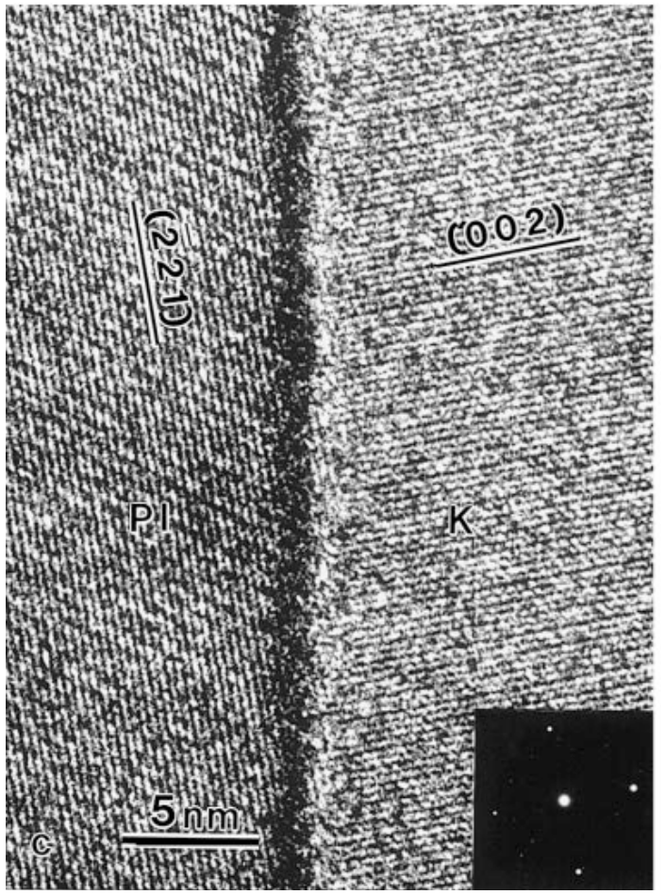

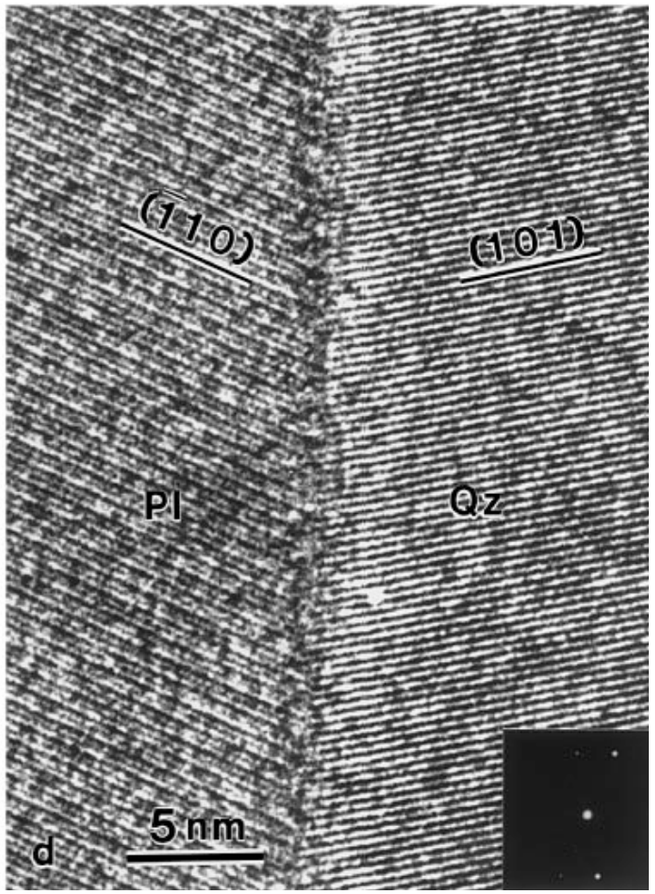

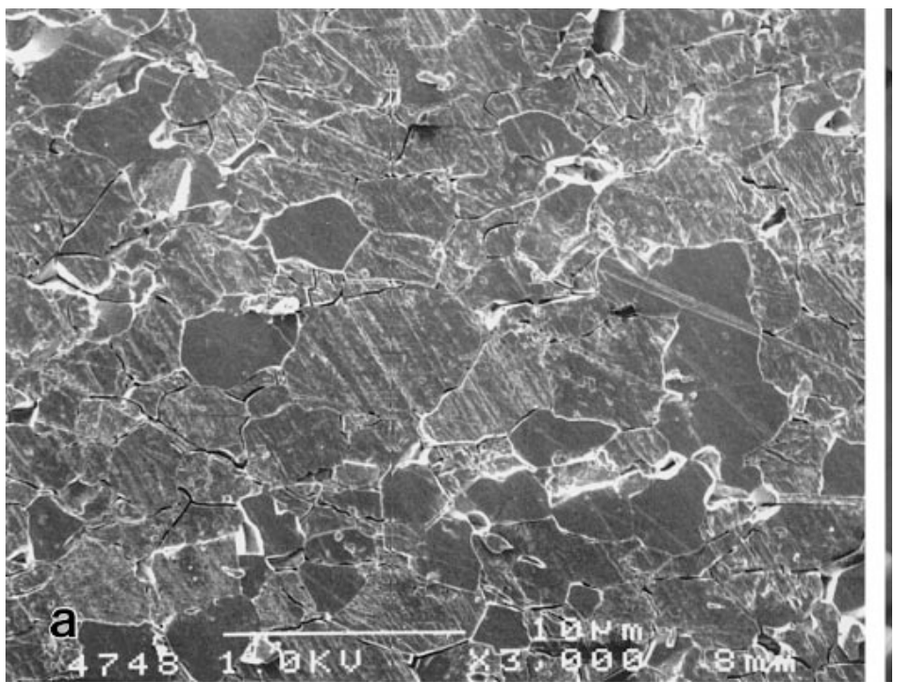

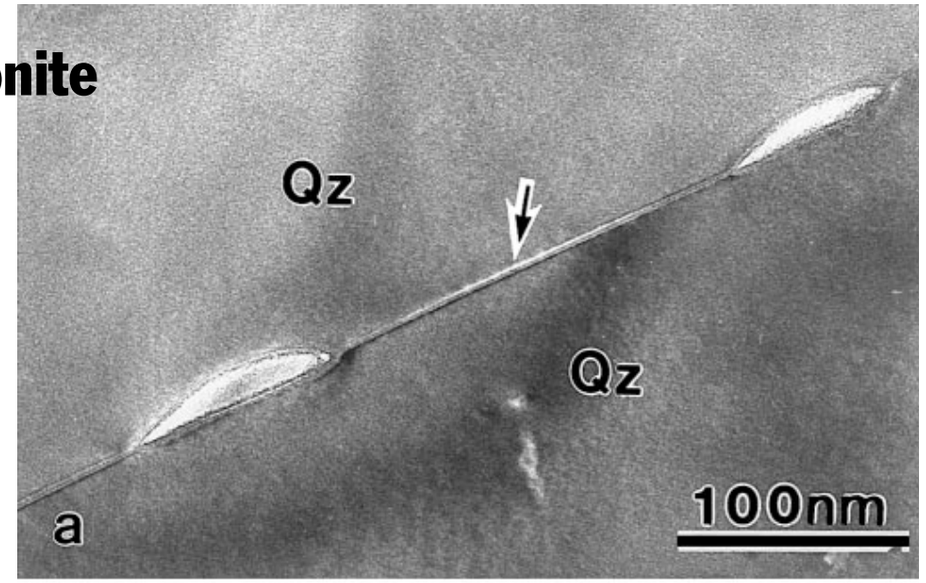

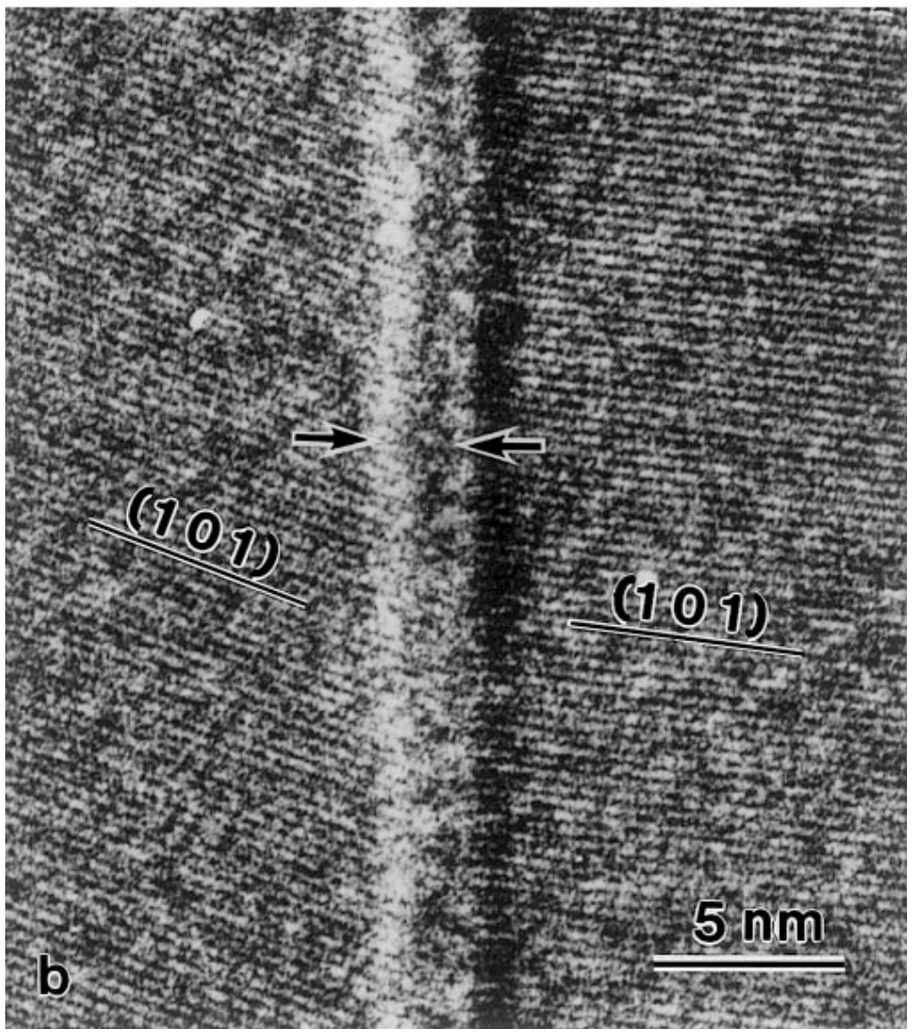

Fig. 6a, b TEM and HREM images of grain boundaries with voids. **a** TEM image of quartz grain boundary with voids. **b** HREM image of the region indicated by an *arrow* in **a**. Both quartz grains are represented by (101) lattice fringes. The boundary has a secondary phase, about 1 nm width with no fringes, as indicated by the *pair of arrows*

Grain boundaries as reservoirs of incompatible elements in the Earth's mantle

Takehiko Hiraga[1]*, **Ian M. Anderson**[2] **& David L. Kohlstedt**[1]

NATURE | VOL 427 | 19 FEBRUARY 2004 | www.nature.com/nature

Figure 1 Chemistry and structure of olivine-olivine grain boundaries in a sample of olivine + anorthite annealed at 1,473 K. **a**, X-ray intensity profile from STEM/EDX analysis for elements in the vicinity of the grain boundaries. The profile is the sum of profiles measured from five grain boundaries. The negative compositional values of trace elements with low concentrations in the olivine grains are indicative of the statistical scatter in the spectral-fitting procedure. **b**, HREM image and diffraction pattern of the olivine grain-boundary area.

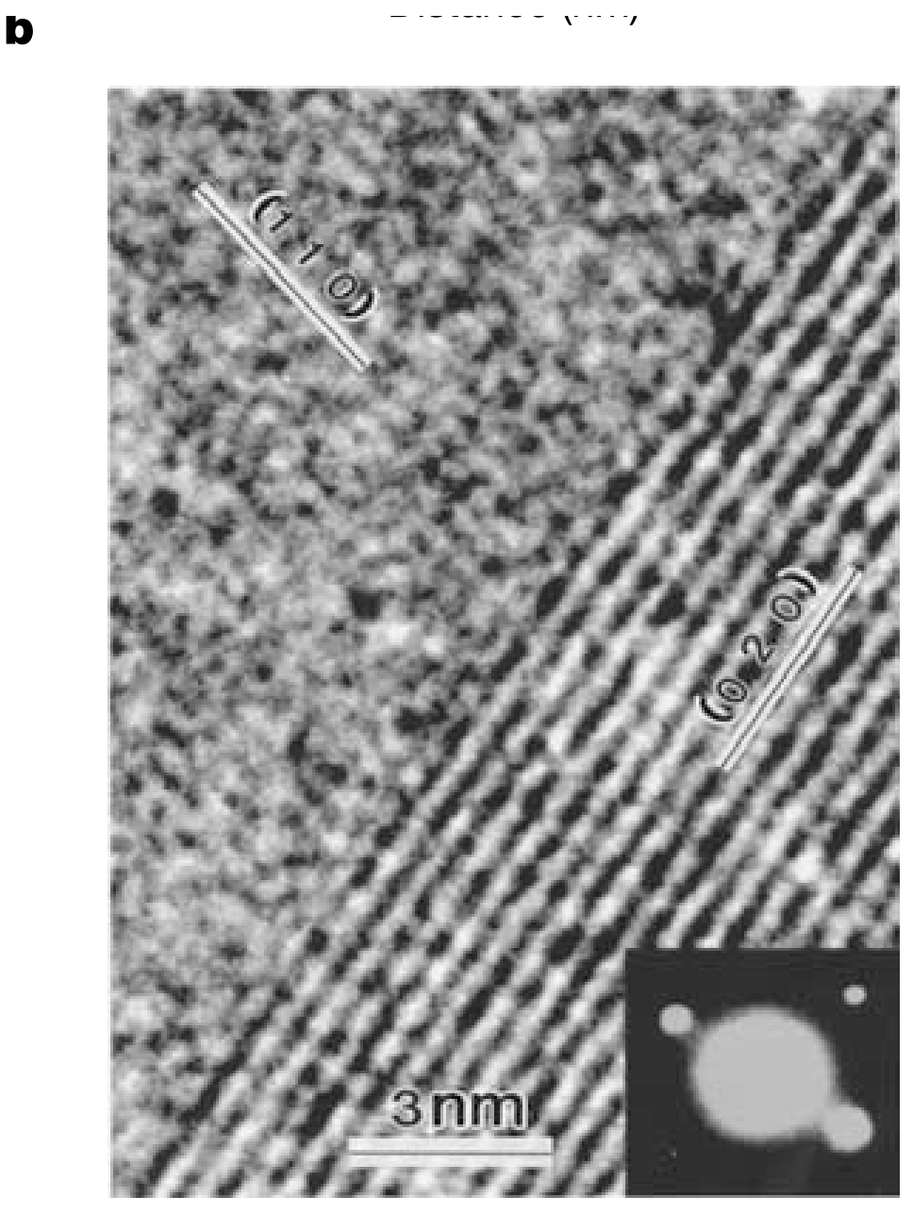

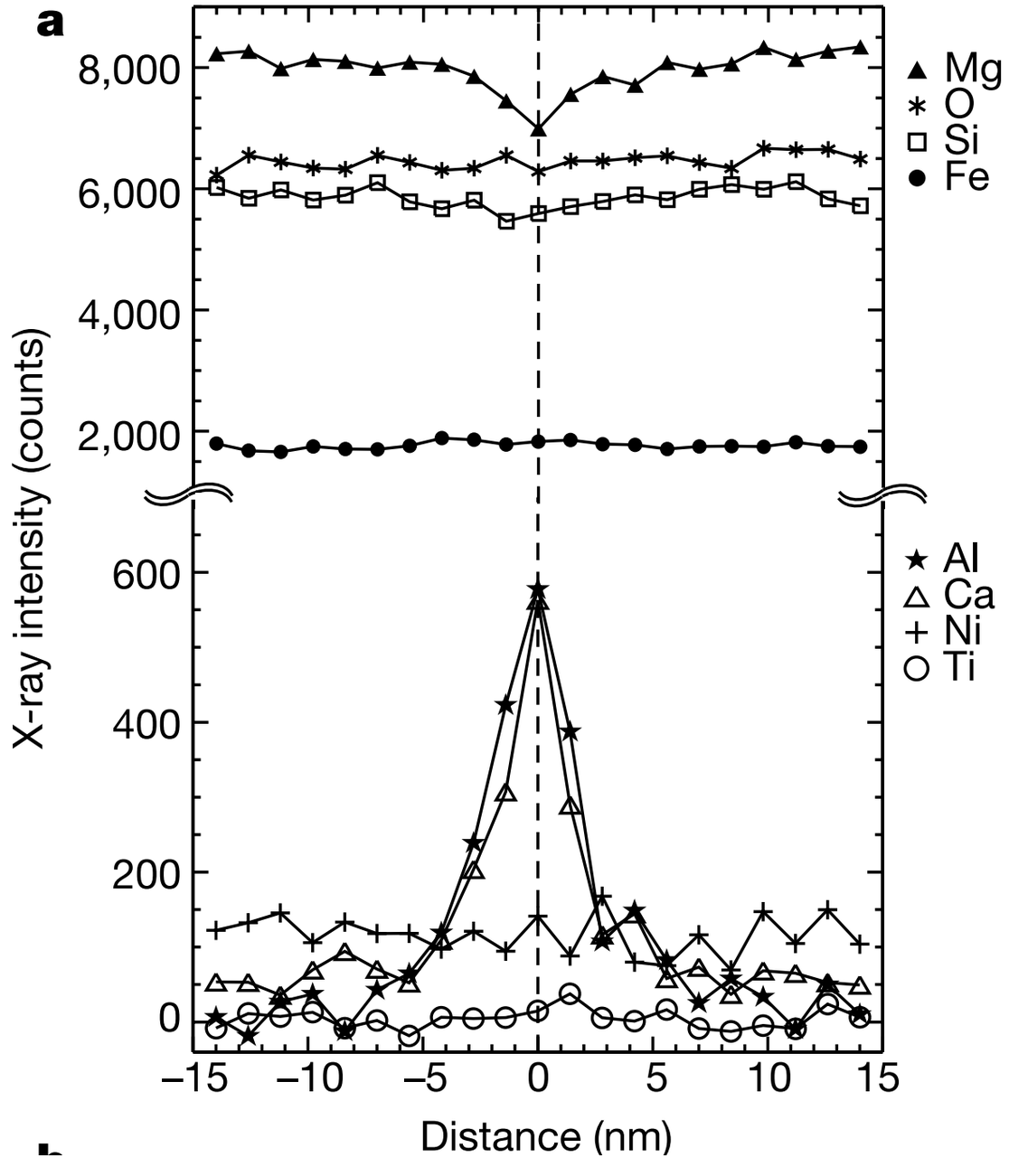

4. Models for diffusion creep at high T

lattice

(Nabarro (1948) Herring(1950):

$$\dot{\varepsilon}_{\mathrm{NH}} = \alpha_{\mathrm{NH}} \frac{\sigma V_{\mathrm{m}}}{RT} \frac{D_{\mathrm{gm}}}{d^2}$$

$$D_{\mathrm{gm}} = D^{\mathrm{o}}_{\mathrm{gm}} \exp\left(- \frac{\Delta E_{\mathrm{gm}} + P\Delta V_{\mathrm{gm}}}{RT} \right)$$

$$= D^{\mathrm{o}}_{\mathrm{gm}} \exp\left(- \frac{\Delta H_{\mathrm{gm}}}{RT} \right)$$

grain boundary

Coble (1963):

$$\dot{\varepsilon}_{\mathrm{C}} = \alpha_{\mathrm{C}} \frac{\sigma V_{\mathrm{m}}}{RT} \frac{\delta D_{\mathrm{gb}}}{d^3}$$

$$D_{\mathrm{gb}} = D^{\mathrm{o}}_{\mathrm{gb}} \exp\left(- \frac{\Delta E_{\mathrm{gb}} + P\Delta V_{\mathrm{gb}}}{RT} \right)$$

$$= D^{\mathrm{o}}_{\mathrm{gb}} \exp\left(- \frac{\Delta H_{\mathrm{gb}}}{RT} \right)$$

combined:

$$\dot{\varepsilon}_{\mathrm{diff}} = 14 \left(\frac{\sigma V_{\mathrm{m}}}{RT} \right) \left(D_{\mathrm{gm}} + \frac{\pi \delta D_{\mathrm{gb}}}{d} \right) \left(\frac{1}{d^2} \right)$$

empirical:

$$\dot{\varepsilon} = A \frac{\sigma^n}{d^m} f^p_{\mathrm{O_2}} f^q_{\mathrm{H_2O}} \exp - \frac{Q_{\mathrm{cr}}}{RT}$$

DIFFUSION-ACCOMMODATED FLOW AND SUPERPLASTICITY*

M. F. ASHBY† and R. A. VERRALL†

ACTA METALLURGICA, VOL. 21, FEBRUARY 1973

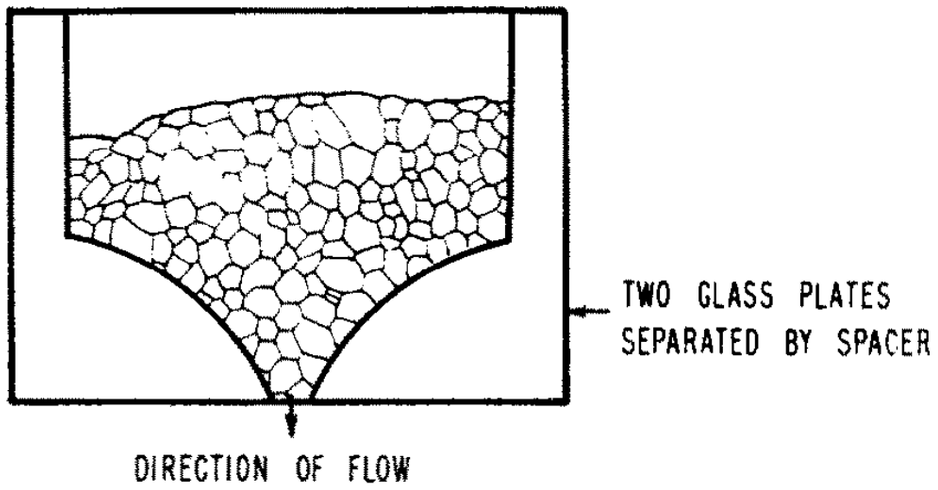

FIG. 2. The cell in which the oil emulsion was deformed. The channel has the shape of a logarithmic spiral.

emulsion:
oil (grains) +
detergent
(grain boundaries)

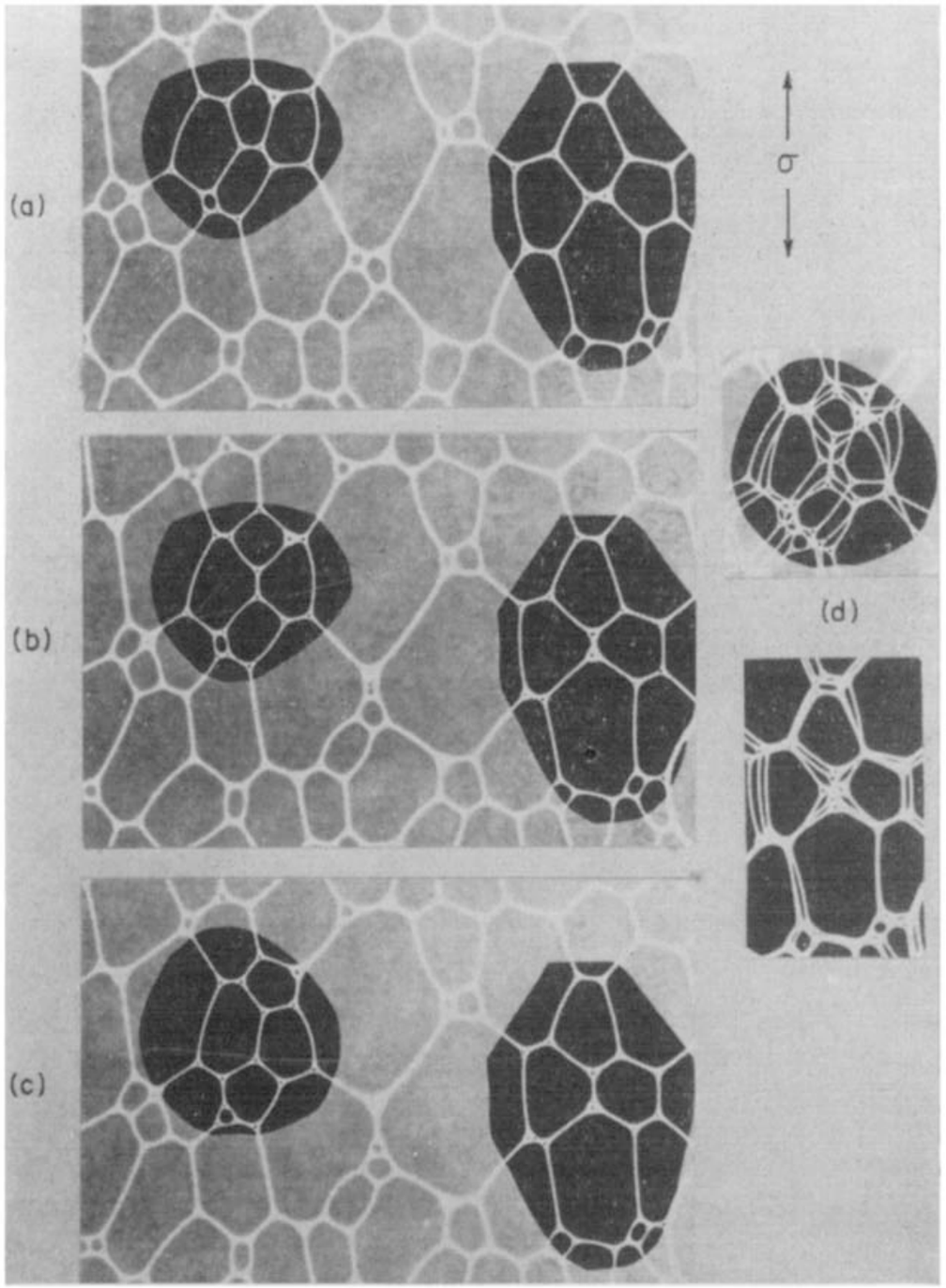

FIG. 5. Photographs (a)–(c) form a sequence in order of increasing strain. Neighbor-switching events have occurred in the areas printed with high contrast. The surroundings relax, transmitting the locally generated strain to the specimen surfaces.

previous models are uniform flow

this is non-uniform flow

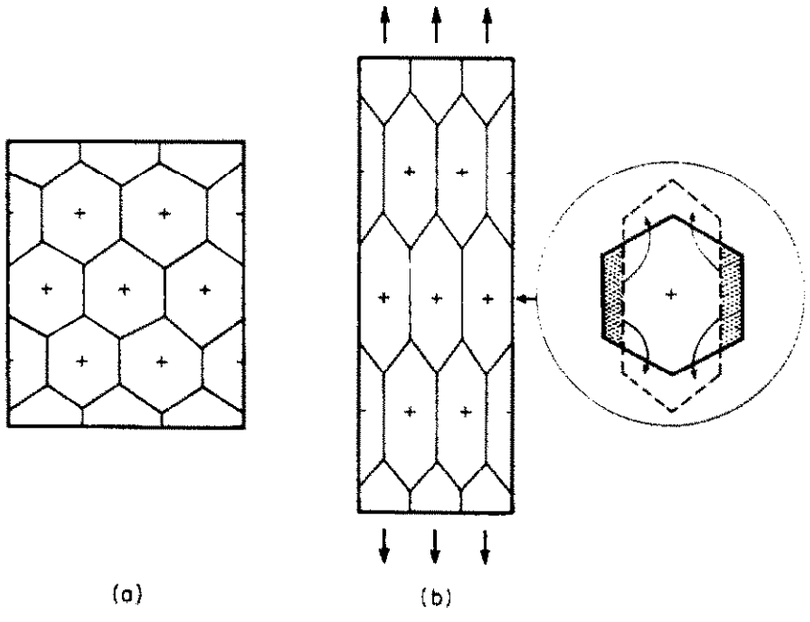

FIG. 1. Quasi-uniform flow. A grain suffers roughly the same shape change as the specimen as a whole and does not switch its neighbors. Dislocation creep, Nabarro–Herring and Coble creep all have these characteristics.

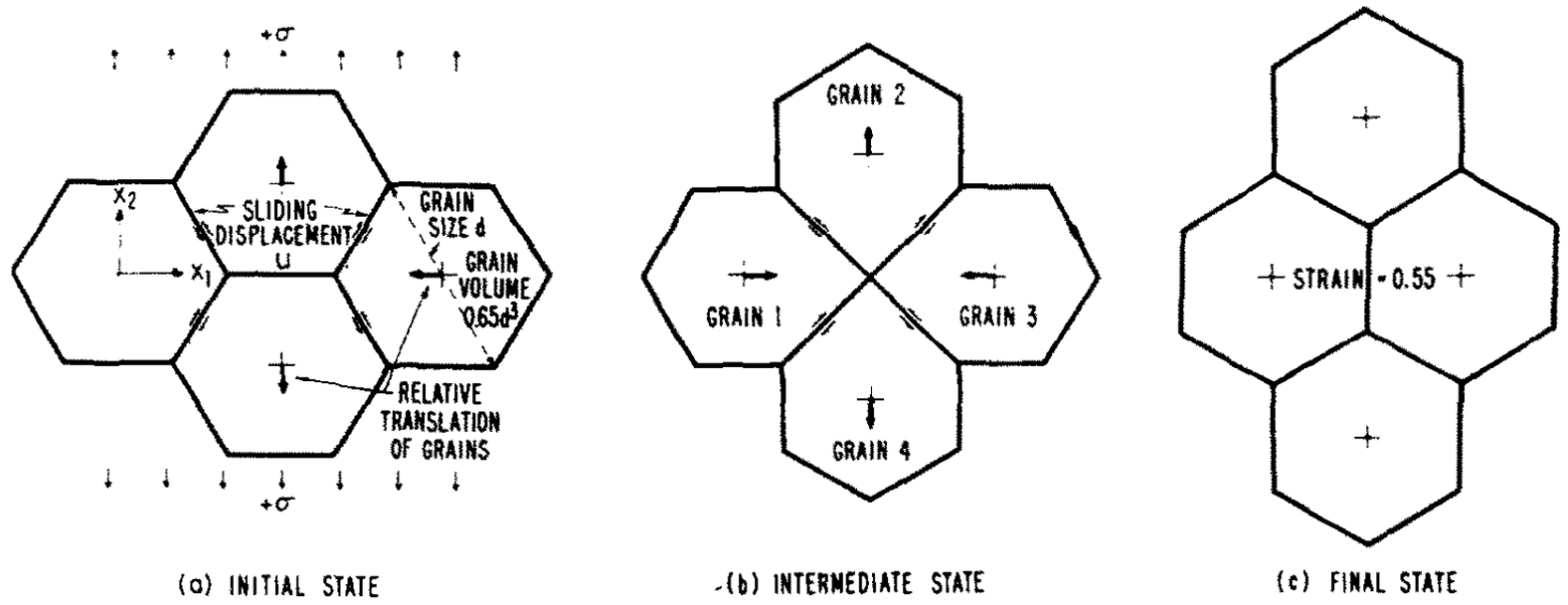

FIG. 4. The unit step of the deformation process. A group of four grains moves from the initial, through the intermediate state to the final state. The initial and final states of the polycrystal are thermodynamically identical, although it has suffered a true strain $\varepsilon_0 = 0.55$. In so doing, the grains suffer accommodation strains and translate

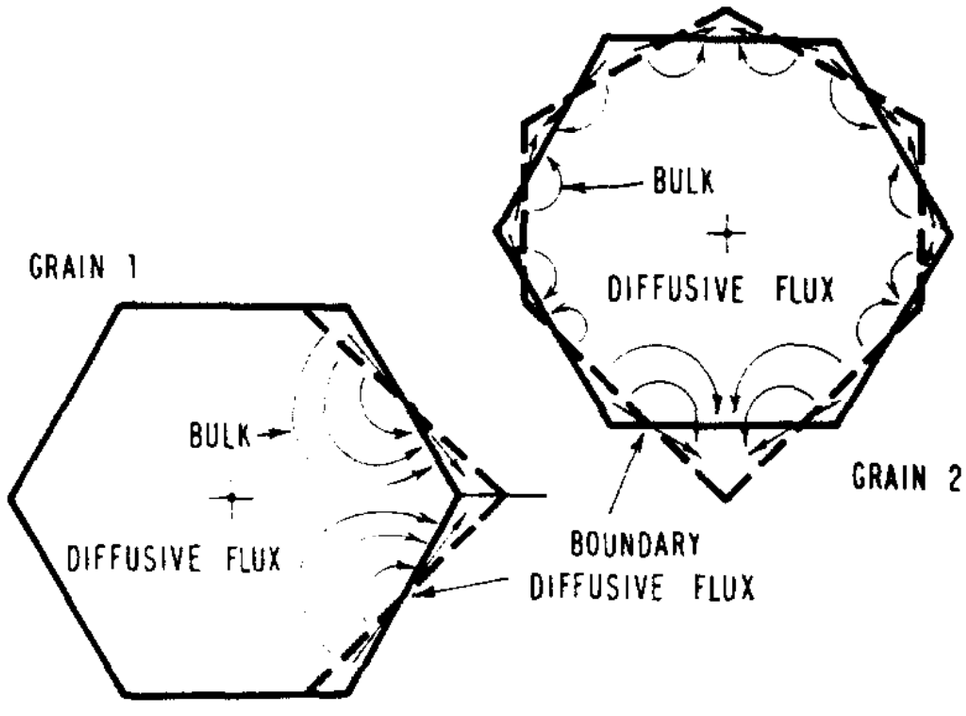

FIG. 7. The accommodation strains required when grains move from the initial to the intermediate states. These may be obtained by bulk diffusion and by boundary diffusion. Note that the flow, particularly in grain 2, is local, confined to the surface regions of the grain.

5. Experimental data (and empirical flow laws)

Influence of water on plastic deformation of olivine aggregates

1. Diffusion creep regime S. Mei & D. Kohlstedt

JOURNAL OF GEOPHYSICAL RESEARCH, VOL. 105, NO. B9, PAGES 21,457–21,469, SEPTEMBER 10, 2000

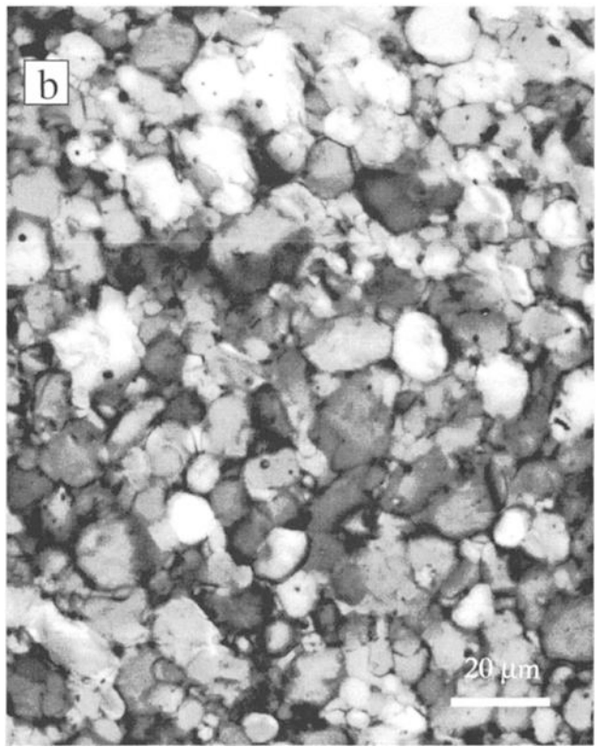

Figure 2. Transmitted plane light photomicrographs of hot-pressed samples: (a) dry sample and (b) wet sample. Scale bar represents 20 μm. These micrographs are from polished and etched sections cut normal to the long axes of the samples.

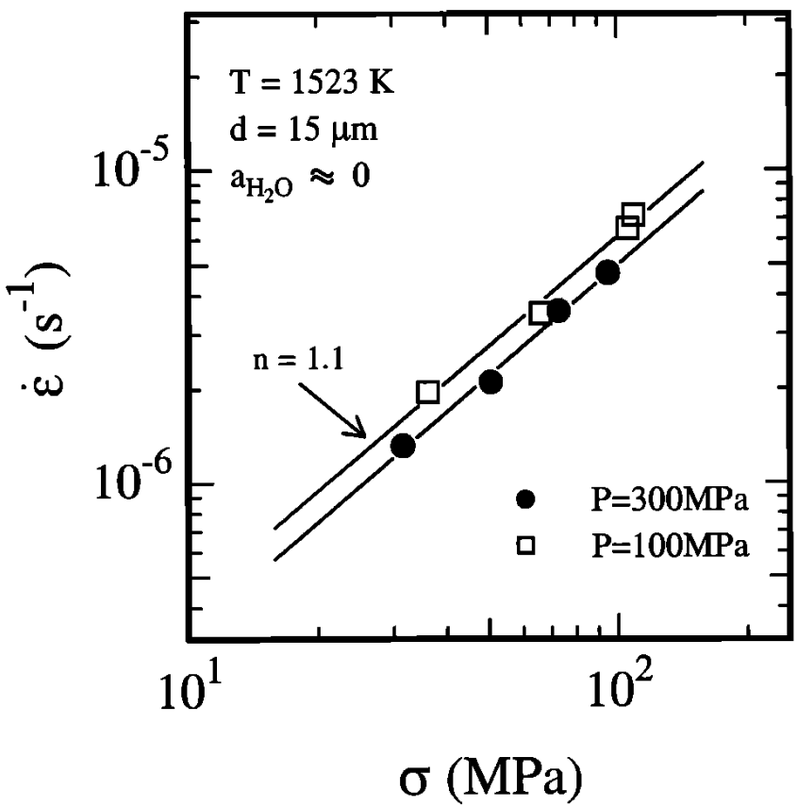

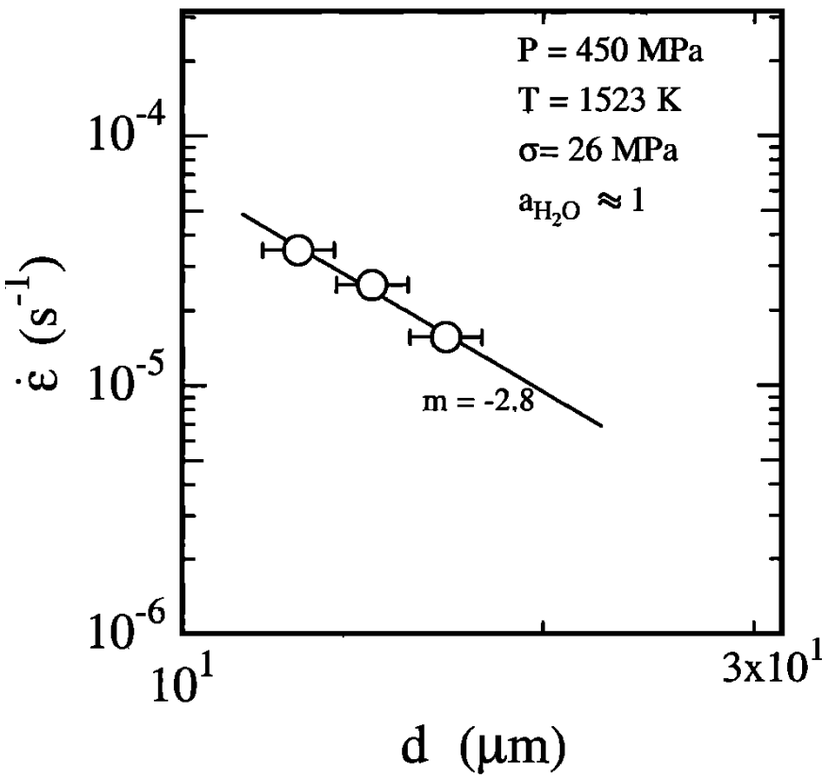

$$\dot{\varepsilon}(\sigma, d, T, P, f_{H_2O}) = A \frac{\sigma^n}{d^p} f_{H_2O}^r \exp\left(-\frac{Q + PV}{RT}\right)$$

6. Effects of water

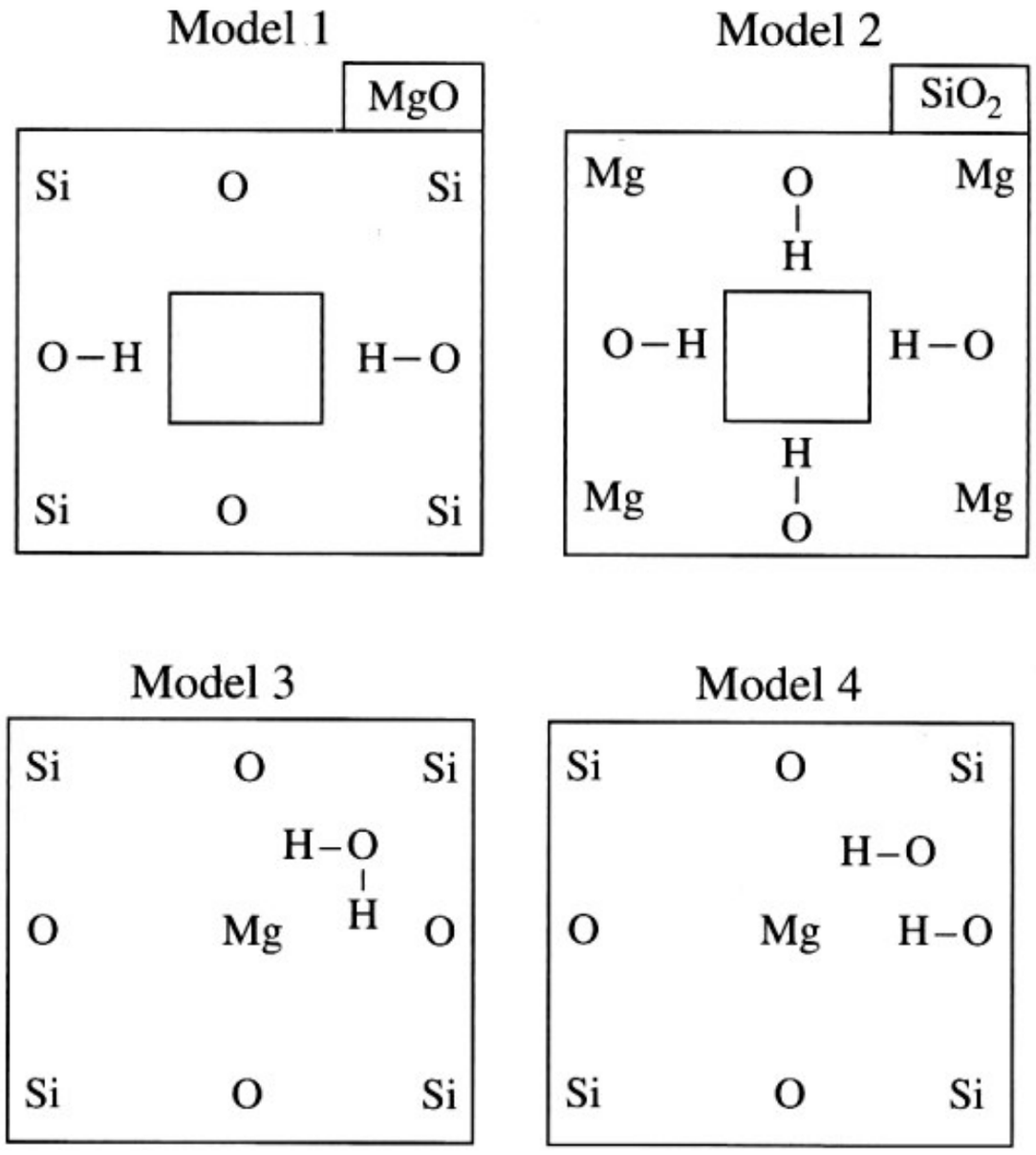

FIGURE 10.5 Mechanisms of dissolution of water in silicate minerals. Hydrogen (proton) and nearby oxygen form an electric dipole. The interaction between an electric dipole and the electromagnetic field (light) causes absorption of light. Note that each mechanism is associated with a specific volume change of a crystal.

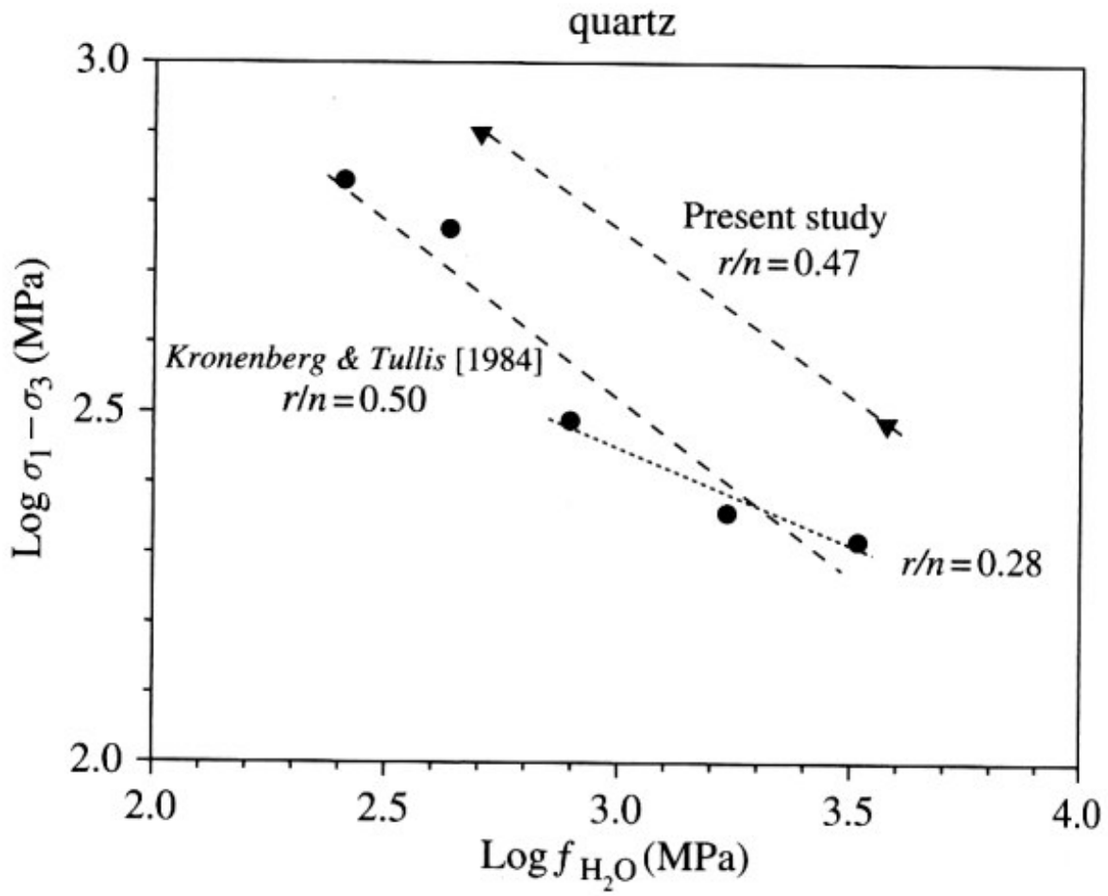

FIGURE 10.8 Dependence of the creep strength of quartz on water fugacity (POST *et al.*, 1996). A constitutive relation of $\dot{\varepsilon} \propto f_{H_2O}^r(P,T) \cdot \sigma^n \cdot \exp\left(-\frac{E^* + PV^*}{RT}\right)$ ($n = 4$) is assumed. The water fugacity is changed by changing the pressure, but the influence of the $\exp(-PV^*/RT)$ term is not included in this analysis (i.e., effectively it is assumed that $V^* = 0$).

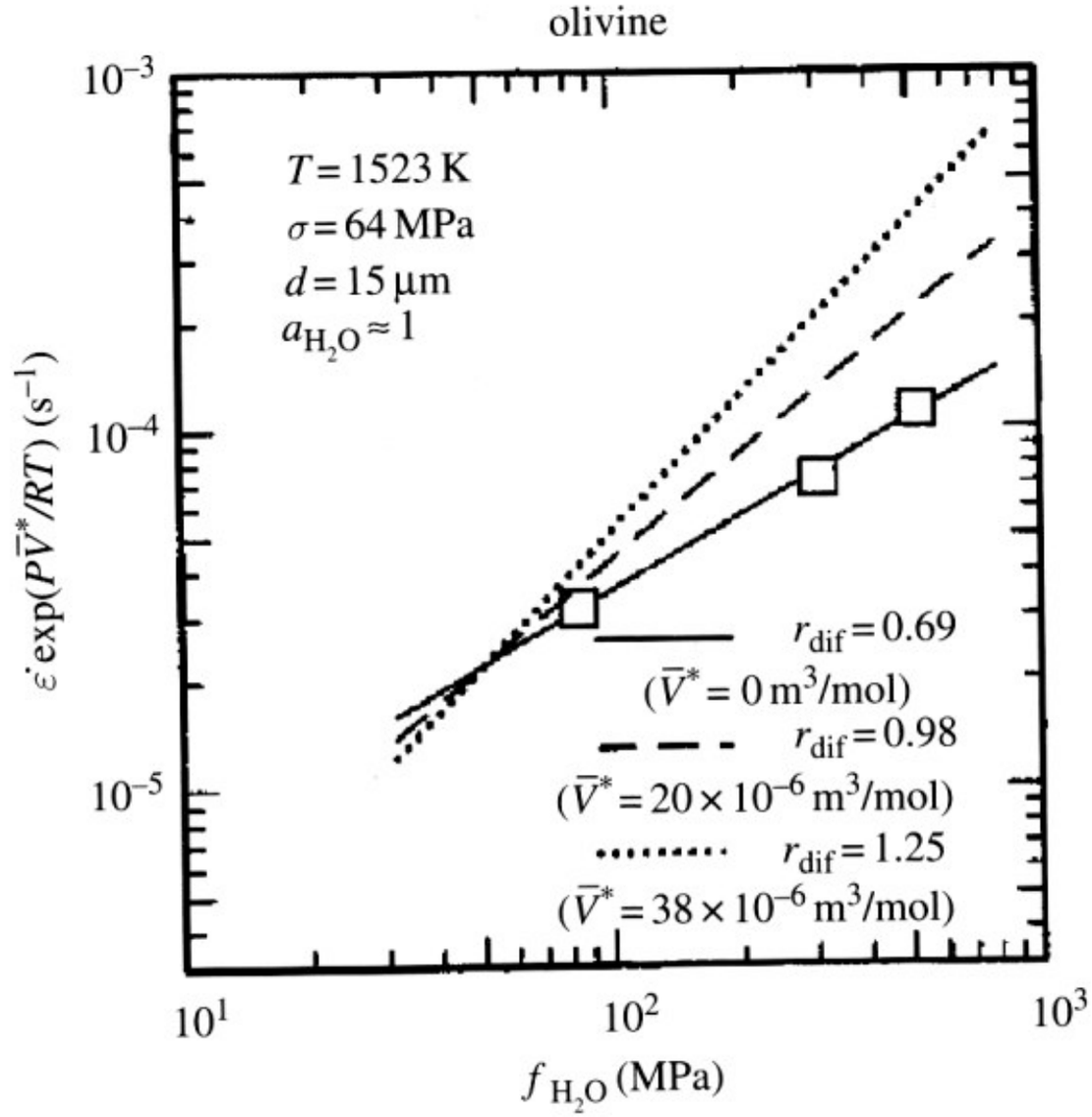

FIGURE 10.9 Influence of water fugacity on the rate of deformation in olivine in the dislocation-creep regime (MEI and KOHLSTEDT, 2000b). In the experiments by MEI and KOHLSTEDT (2000b), the water fugacity was changed by changing the total confining pressure. Consequently, the value of the water fugacity exponent, r, cannot be determined uniquely because it depends on the unknown activation volume $\bar{V}^*$ (for details see the later part of this chapter).

7. Effects of melt

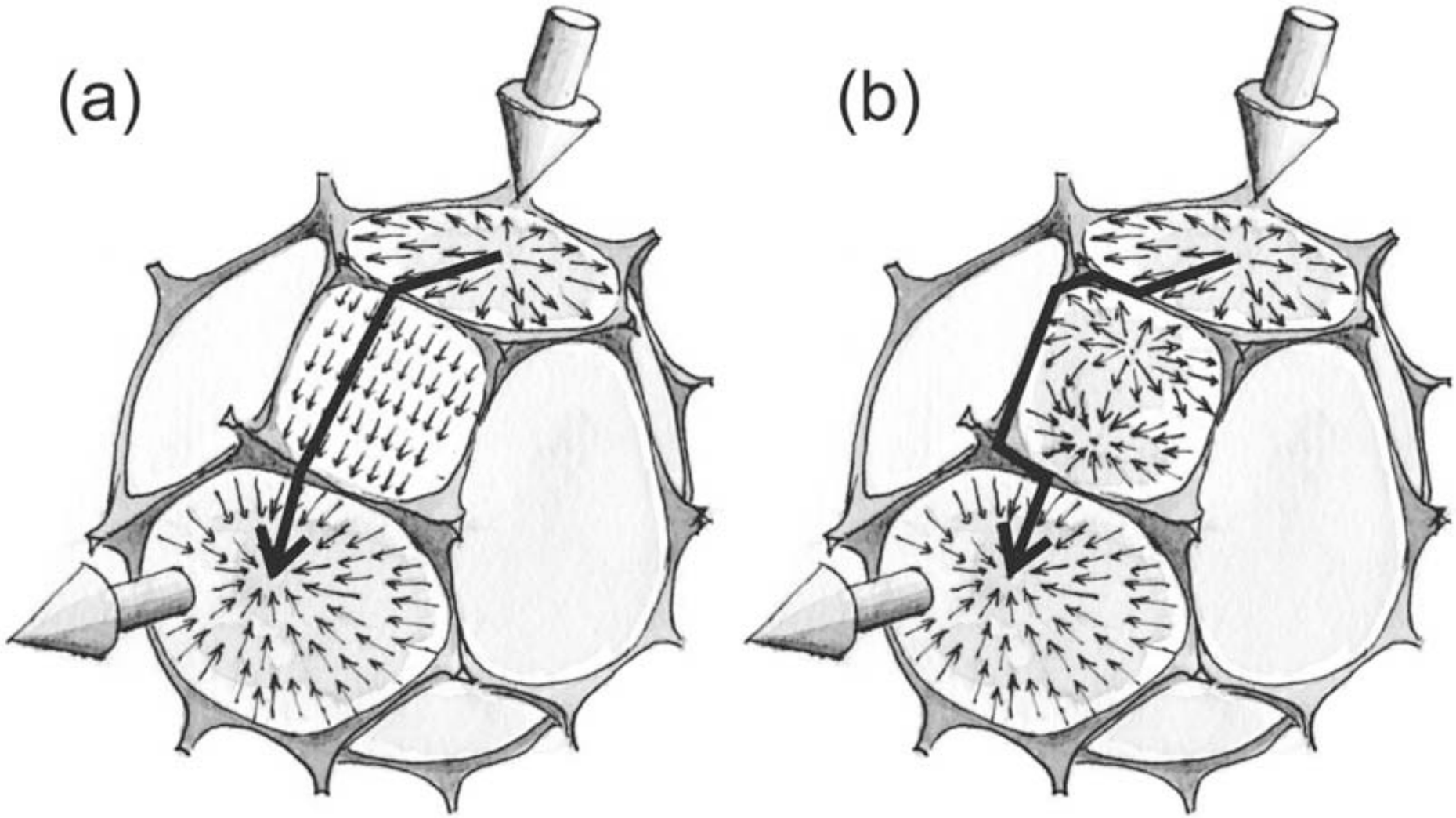

Figure 5. Schematic illustration showing the significant difference in the diffusion paths between (a) CK model and (b) contiguity model, under shear deformation shown by 3-D arrows. Thick arrows show the quasi-2-D approximation of the 3-D diffusion paths.

(a)

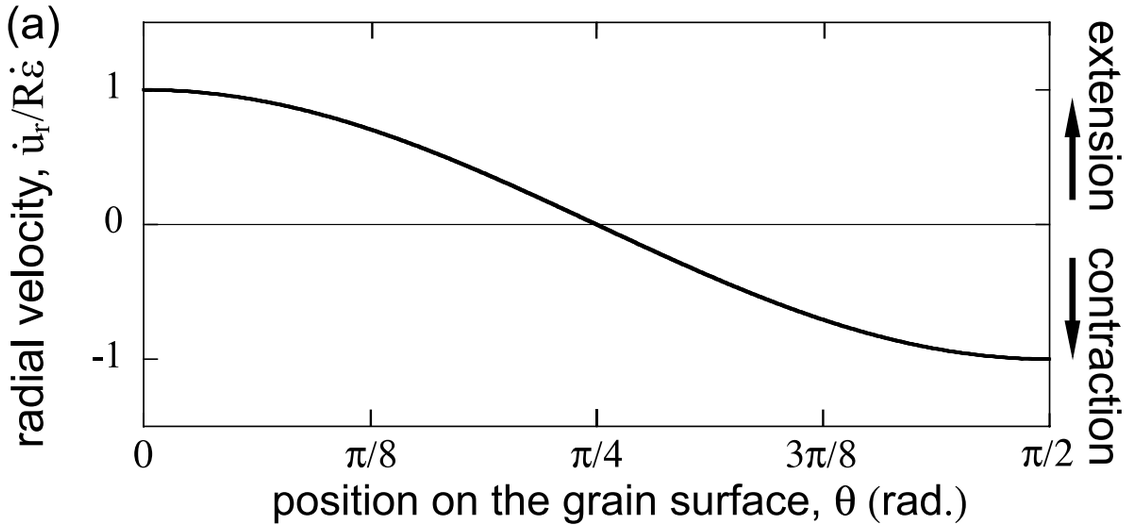
radial velocity, $\dot{u}_r/R\dot{\varepsilon}$
1
0
-1
0
π/8
π/4
3π/8
π/2
position on the grain surface, θ (rad.)
extension
contraction

(b)

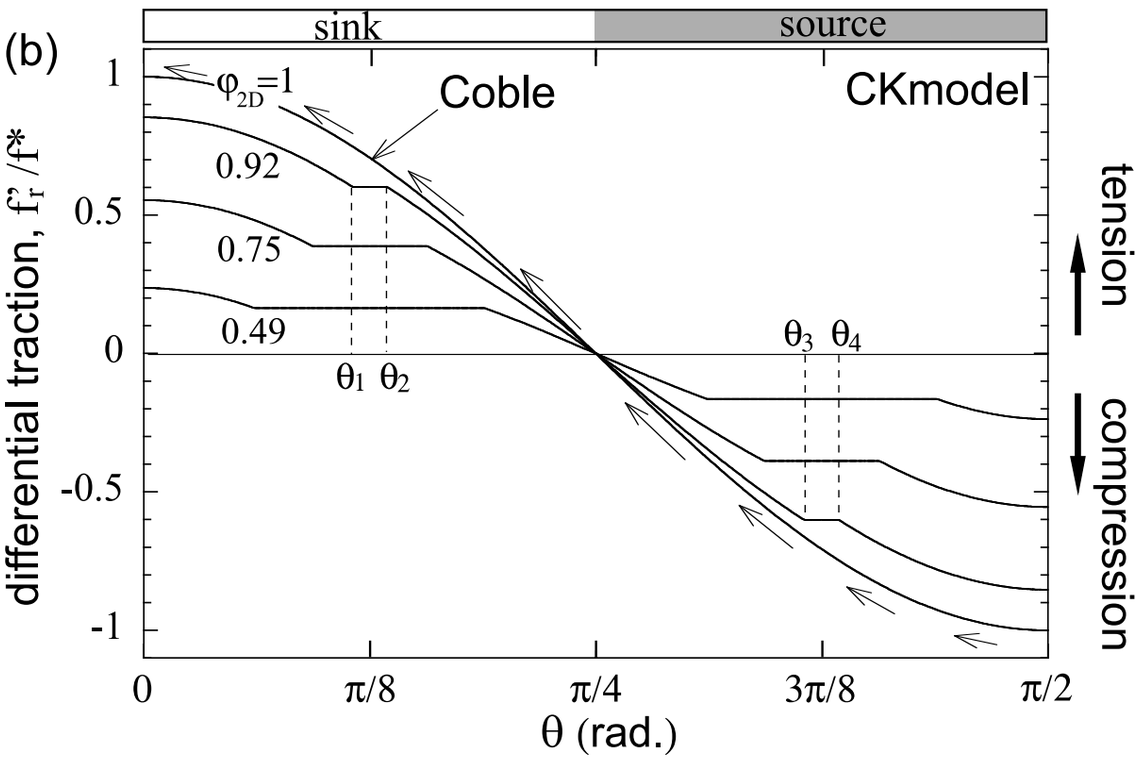
sink
source
differential traction, f_r'/f^*
1
0.5
0
-0.5
-1
φ_{2D}=1
0.92
0.75
0.49
Coble
CKmodel
θ_1 θ_2
θ_3 θ_4
0
π/8
π/4
3π/8
π/2
θ (rad.)
tension
compression

(c)

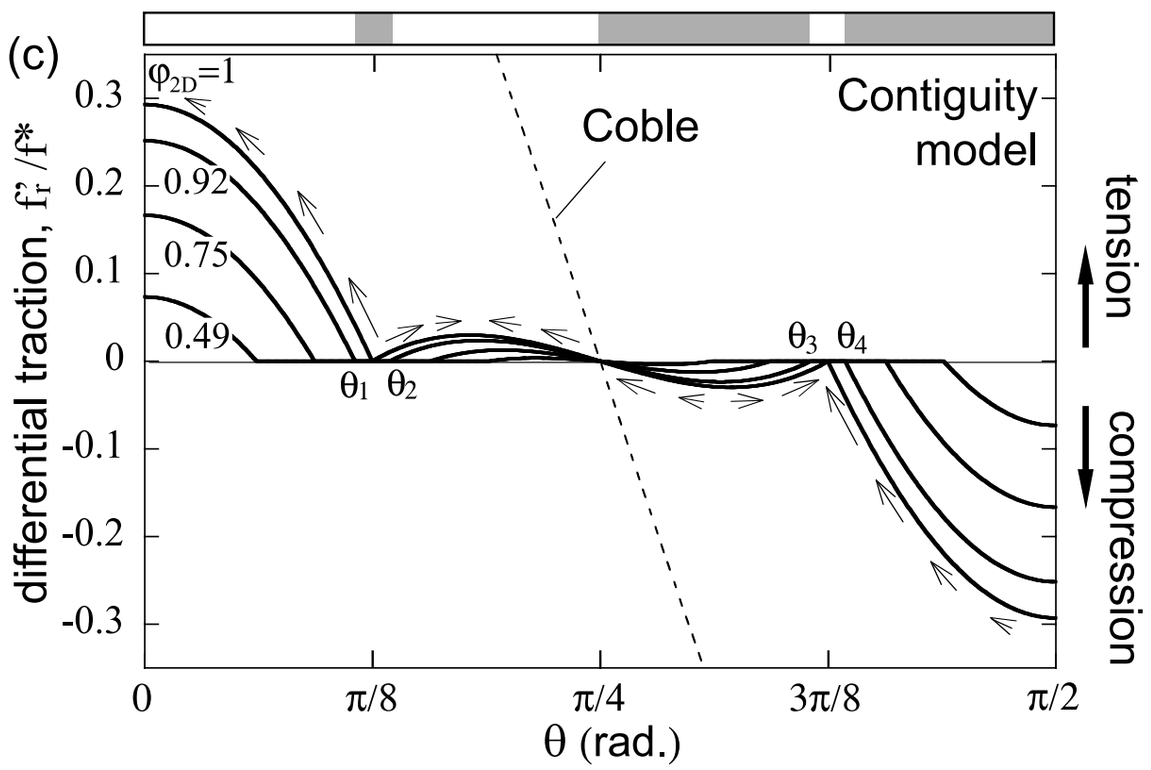
differential traction, f_r'/f^*
0.3
0.2
0.1
0
-0.1
-0.2
-0.3
φ_{2D}=1
0.92
0.75
0.49
Coble
Contiguity model
θ_1 θ_2
θ_3 θ_4
0
π/8
π/4
3π/8
π/2
θ (rad.)
tension
compression

Viscosity as a function of contiguity

and melt fraction at textural equilibrium

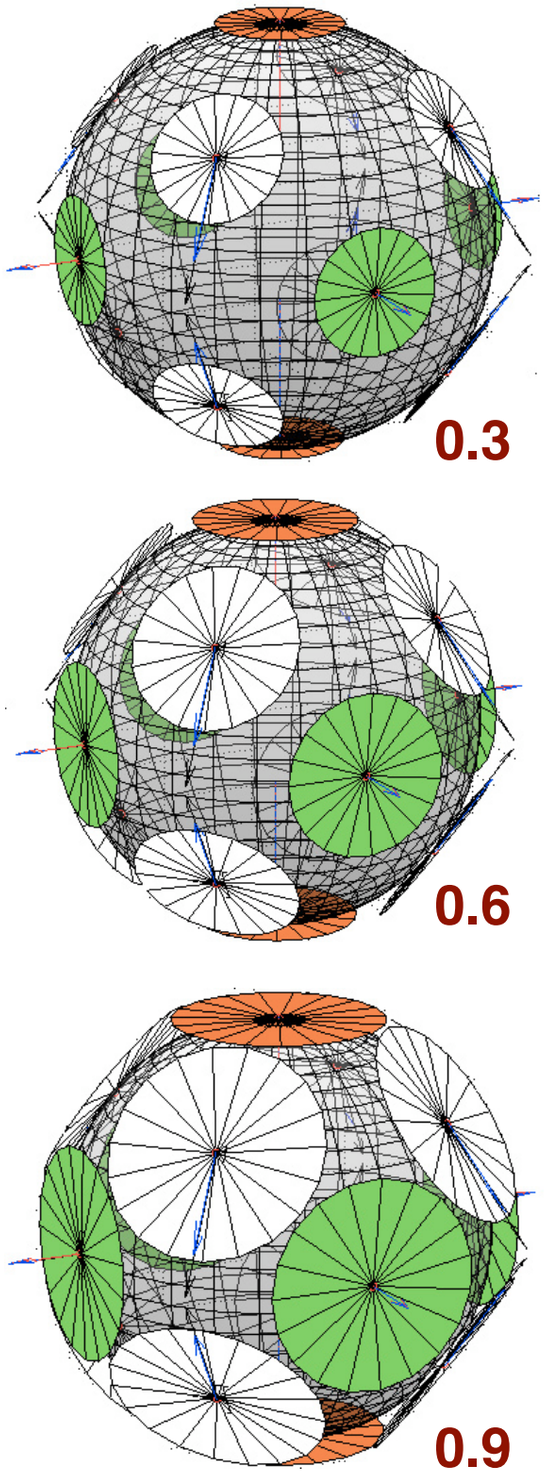

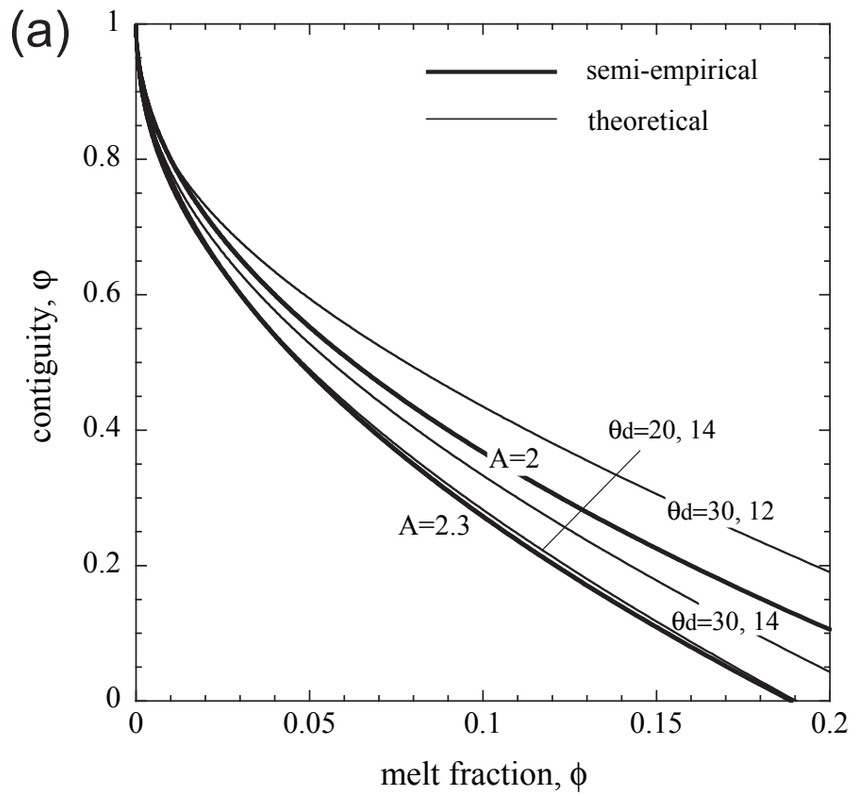

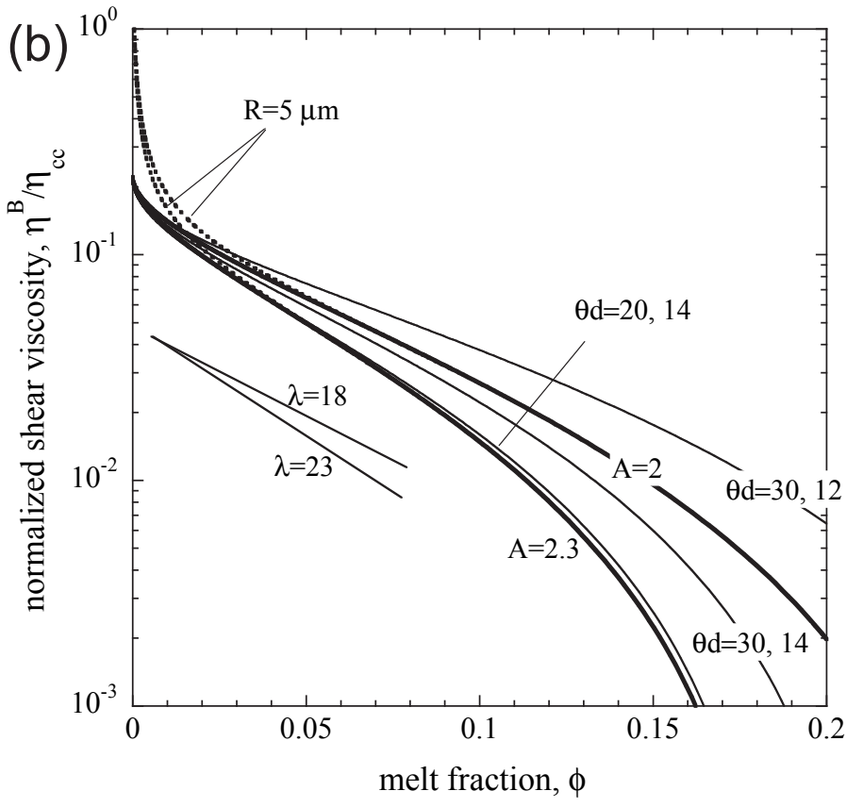

Summary

1. Diffusion is a random walk process of vacancies, coupled to atoms. To change the shape of a grain, the diffusion is driven by stress gradients.

2. The rate (kinetics) of shape change depend on the diffusion path and its diffusivity that contribute to the flux of atoms. The diffusivity depends strongly on T (the thermally activated process is the jump frequency).

3. Diffusion Creep, from models and experimental result has a non-linear dependence on grain size (d^(-2-3)) and a linear dependence on stress.

4. High strains are achieved by grain switching, requiring grain boundary sliding and less strain per grain (can be referred to as “superplasticity”).

5. Water aids diffusion by weakening bonds and/or by increasing the number of vacancies.

6. Melt aids diffusion by reducing diffusion path lengths if the porosity is connected.

A new model for grain-boundary diffusion creep with melt

Takei and Holtzman, 2009a., (based on Cooper-Kohlstedt model)

$$\sigma_{ij}^{S} + p^{L}\delta_{ij} = [C_{ijkl}^{\mathrm{vi}}]\dot{\varepsilon}_{kl}$$

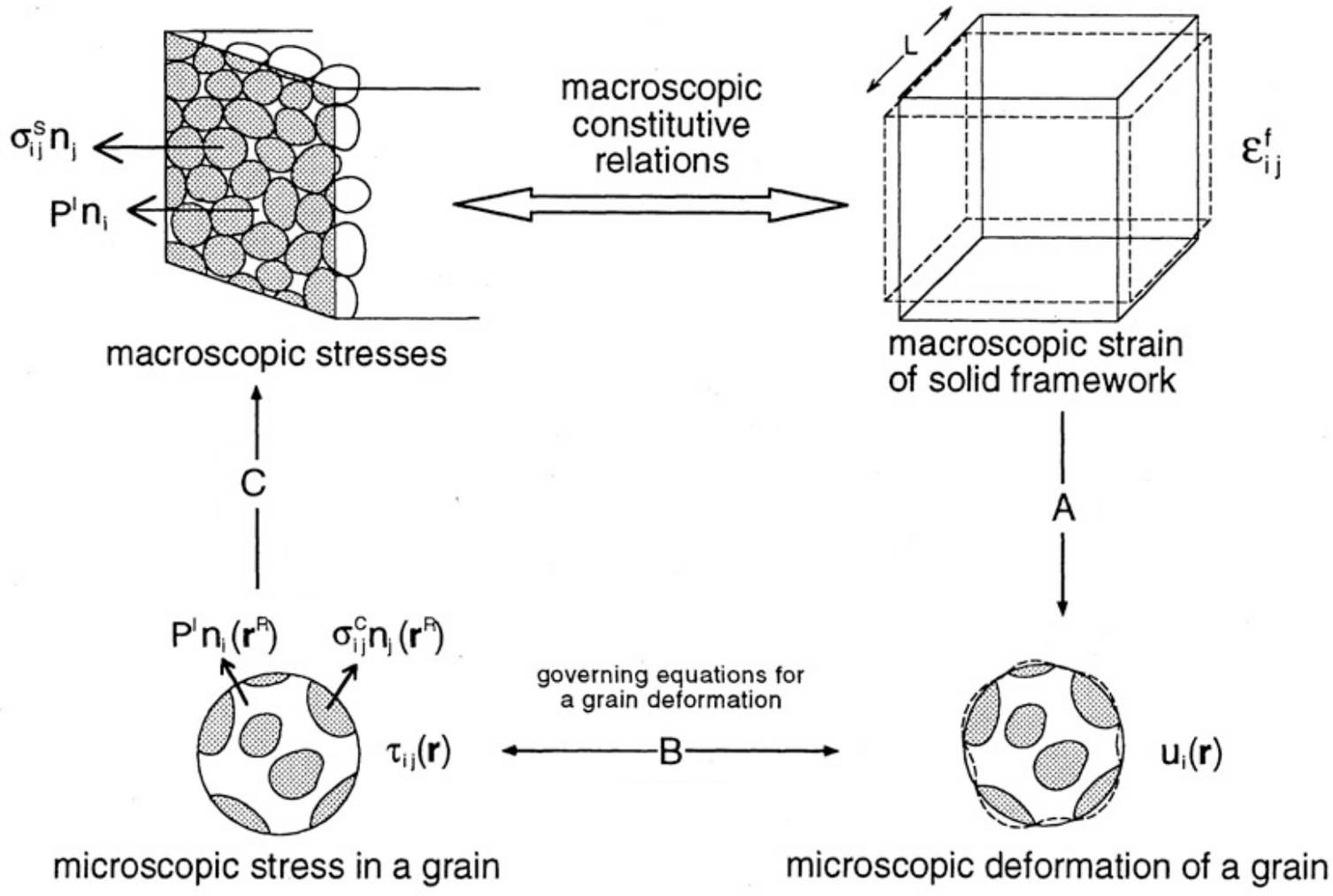

now in steady state, small strain limit

$$C_{ijkl}^{\mathrm{vi}} = \frac{(1-\phi)3RT(d/2)^3}{32D\delta\Omega}\sum_{f=1}^{\mathrm{nf}}\left(\frac{a_f}{d/2}\right)^4 n_i^f n_j^f n_k^f n_l^f \qquad \frac{\partial \tau_{ij}}{\partial x_j} = 0 \quad \mathrm{at} \quad r < R$$

Grain Boundary Diffusion creep (from Cooper-Kohlstedt / Coble creep model)

symbol	
J	matter flux $(mol/m^2/s)$
J_v	vacancy flux $(mol/m^2/s)$
C_v	mole fraction of vacancies in grain boundary (GB).
Ω	molar volume of matter or vacancy (m^3/mol)
P	normal traction on the surface, compression positive (Pa)
ΔP	variation from P°
N_v	number of vacancies by mole per unit volume of GB (mol/m^3)
U_v	formation energy of a vacancy (J/mol)
N	number of matter (atoms) in moles per unit volume of GB (mol/m^3)
N_v	$= NC_v$, number of moles of vacancies
D_v	diffusivity of vacancy (m^2/s)
D	$= C_v D_v$, diffusivity of matter (m^2/s)

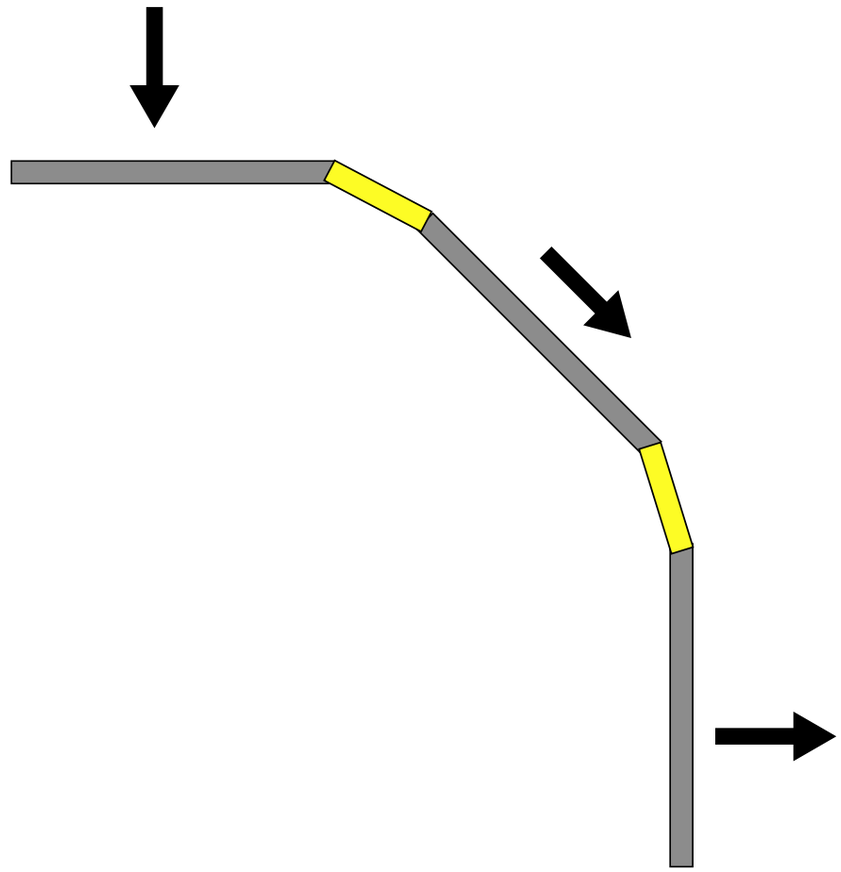

Mass conservation

$$-\nabla \cdot J = \frac{\dot{u}_r}{\delta\Omega}$$

Mass balance

$$J = -J_v$$

Vacancy flux

$$J_v = -D_v \cdot \nabla N_v$$

and the definition of N

$$N_v = NC_v = N \exp\left(-\frac{U_v + P\Omega}{RT}\right)$$

linearize the exponential term by the approximation
$C_v = C_v^\circ(1 - \frac{\Delta P\Omega}{RT})$ and $C_v^\circ = \exp -(\frac{U_v + P^\circ\Omega}{RT})$;

Combining the first three gives

$$\nabla \cdot \nabla N_v = -\frac{\dot{u}_r}{\delta\Omega D_v}$$

$$\nabla \cdot \nabla P = \frac{RT}{NC_v\Omega^2\delta D_v}\dot{u}_r$$

Then solve this

$$\Delta F = P - P_L$$

$$\Delta F^f = -\left(\frac{\pi RT}{8D\delta\Omega}\right)\dot{u}_r^f (a_f)^4$$

$$\Delta F^f = -\dot{u}_r^f (a_f)^4$$